

INTERNATIONAL JOURNAL OF
Robust and Nonlinear Control

**Discrete gain scheduling control approach to elliptical orbit
rendezvous system with actuator saturation**

Journal:	<i>International Journal of Robust and Nonlinear Control</i>
Manuscript ID	RNC-22-0557.R1
Wiley - Manuscript type:	Research Article
Date Submitted by the Author:	03-Oct-2022
Complete List of Authors:	Yang, Hongfu; Guangxi Normal University Gao, Xiangyu; Guangxi Normal University 1, 1 Dongyan He; Guangxi Normal University Teo, Kok Lay; Sunway University Jianqiao, Wang; Guangxi Normal University
Keywords:	Spacecraft rendezvous, periodic Riccati equation, discrete scheduling control approach, actuator saturation, invariant set
<p>Note: The following files were submitted by the author for peer review, but cannot be converted to PDF. You must view these files (e.g. movies) online.</p> <p>WileyNJD-v2.cls NJDnatbib.sty wileyNJD-AMA.bib</p>	

SCHOLARONE™
Manuscripts

<http://mc.manuscriptcentral.com/rnc-wiley>

This is the author manuscript accepted for publication and has undergone full peer review but has not been through the copyediting, typesetting, pagination and proofreading process, which may lead to differences between this version and the [Version of Record](#). Please cite this article as doi: [10.1002/rnc.6509](https://doi.org/10.1002/rnc.6509)

This article is protected by copyright. All rights reserved.

Author Manuscript

1
2
3
4 The main contributions of this paper are stated as follows:
5
6

- 7 a) By rotation (reflection) transformation technique, a novel time-
8 invariant elliptic invariant set is constructed to determine the switching
9 points of the discrete gain scheduling control.
10
11
12
13
14 b) Since T-H equations can be transformed into linear periodic system,
15 the discrete gain scheduling control approach is chosen to make use for
16 the periodicity of the system, i.e., the discrete parameters of this
17 approach can preserve the periodicity of the solution of the periodic
18 Riccati equation.
19
20
21
22
23
24
25
26
27
28 c) Different from the static gain scheduling control approach, the discrete
29 gain scheduling control approach can improve the dynamic
30 performance of the system under input saturation.
31
32
33
34
35
36
37
38
39
40
41
42
43
44
45
46
47
48
49
50
51
52
53
54
55
56
57
58
59
60

RESEARCH ARTICLE

Discrete gain scheduling control approach to elliptical orbit rendezvous system with actuator saturation

Xiangyu Gao¹ | Dongyan He¹ | Kok Lay Teo² | Jianqiao Wang¹ | Hongfu Yang¹¹School of Mathematics and Statistics, Guangxi Normal University, Guilin, China²School of Mathematical Sciences, Sunway University, Bandar Sunway, Selangor Darul Ehsan, Malaysia**Correspondence**

Hongfu Yang, School of Mathematics and Statistics, Guangxi Normal University, Guilin, Guangxi, 541004, China. Email: yanghf783@nenu.edu.cn

Abstract

This paper studies the discrete gain scheduling control design problem of elliptical orbit spacecraft rendezvous system with actuator saturation. Due to the presence of actuator saturation, the dynamic performance of the spacecraft rendezvous system degrades significantly. In order to improve the dynamic performance of the system, a discrete gain scheduling control approach is adopted to construct a group of time-invariant ellipsoidal invariant sets, which can be used to determine the switching points of the discrete gain scheduling control. By choosing some discrete parameter values, the discrete gain scheduling control is obtained from a solution of a periodic Riccati matrix differential equation. Under the control obtained, the dynamic performance of the system is much improved while accomplishing successfully the rendezvous mission of the spacecraft. Finally, a practical example is provided to show the effectiveness of the proposed control design approach.

KEYWORDS:

Spacecraft rendezvous, periodic Riccati equation, discrete gain scheduling control, actuator saturation, invariant set

1 | INTRODUCTION

Spacecraft rendezvous has been regarded as an important mission in aerospace engineering such as space stations, space laboratories, space communication and remote sensing platforms. Successful rendezvous is a precondition for many space missions, including interception, rescue, repair, docking, large-scale structure assembly and satellite networking. During the past few decades, many spacecraft rendezvous control problems have been studied based on linear time-invariant Hill-Clohessy-Wiltshire (H-C-W) equations¹. However, results on linear time-varying Tschauner-Hempel (T-H) equations² are rare. This is mainly because T-H equations has the time-varying features such that the spacecraft rendezvous control problems are much more complicated. This is the motivation for the study being carried out in this paper.

Due to the limitation of thrust equipment and limited engine power, no real actuator can provide unlimited control force^{3,4,5}. Thus, there is always input saturation in the spacecraft rendezvous system. If the input saturation in the control design is ignored, it may cause system performance to deteriorate, and in the worst case the system may become unstable. Hence, it is necessary to take into account input saturation in the spacecraft rendezvous system. Many advanced approaches have been used to study spacecraft rendezvous control problems with input saturation.

2
3
4
5
6
7
8
9
10
11
12
13
14

For example, the linear matrix inequality (LMI) approach was applied in References^{6,7,8} to solve the robust H_∞ control problem of spacecraft rendezvous system with input constraint. An adaptive sliding mode control approach was proposed in Reference⁹ to study the maneuver of spacecraft rendezvous with input saturation, where system parameters are unknown. In Reference¹⁰, a robust composite nonlinear feedback control approach was utilized to design an orbital controller for the spacecraft rendezvous system under the conditions of parameter uncertainty, external disturbances, and input saturation. In References^{11,12,13,14}, the periodic Lyapunov equation approach was applied to solve the spacecraft rendezvous control problem with control constraints. In Reference¹⁵, the periodic Riccati equation approach was utilized to accomplish elliptical spacecraft rendezvous under control magnitude constraints and energy saturation. It is noted that the results obtained under input saturation mentioned above show that the dynamic performance of the spacecraft rendezvous system will deteriorate in the presence of input saturation. Therefore, the control design strategy is of great importance to improve the dynamic performance of the input-saturated spacecraft rendezvous system. This is the main motivation of this paper.

15
16
17
18
19
20
21
22
23
24
25
26
27
28
29
30

The gain scheduling control approach is one of the most important nonlinear control approach. This approach includes the static gain scheduling control approach, the continuous gain scheduling control approach and the discrete gain scheduling control approach. These approaches have been widely employed in the study of input-saturated spacecraft rendezvous system. For example, a static gain scheduling control approach was used in Reference¹⁶ to design the static gain control for the spacecraft rendezvous system subject to input saturation. Note that although the static gain scheduling control can satisfy input saturation requirement, the dynamic performance of the spacecraft rendezvous system can be less satisfactory. In order to solve this problem, a continuous gain scheduling control approach is utilized in Reference¹⁷ to enhance^{17,18,19,20,21,22} the dynamic performance of the spacecraft rendezvous system subject to input saturation. In addition, a discrete gain scheduling control approach was also adopted in References^{18,19,20,21,22} to improve the dynamic performance of the spacecraft rendezvous system with input saturation. From the above literature, it appears that the dynamic (continuous and discrete) gain scheduling control approach has only been applied to improve the dynamic performance of the spacecraft rendezvous system described by H-C-W equations. However, this approach cannot be applied directly to the spacecraft rendezvous system described by T-H equations due to its time-varying characteristics. This paper aims to study how to apply this approach to the spacecraft rendezvous problem described by T-H equations.

31
32
33
34
35
36
37
38
39
40
41

In nonlinear control theory, invariant set is a very important concept, which is usually characterized by the level set of Lyapunov function. Since the domain of attraction of a nonlinear system cannot be accurately described, invariant set can be used to estimate the domain of attraction of a nonlinear system^{23,24,25}. For example, it has been applied to estimate the domain of attraction of a spacecraft rendezvous system. For the time-invariant H-C-W equations under input saturation, it is easy to obtain directly an invariant set through the level set of the Lyapunov function. However, for the time-varying T-H equations under input saturation, direct construction of an invariant set from the level set of the Lyapunov function is not possible due to the time-varying characteristics of T-H equations. The aim of this paper is to develop a novel approach to construct an invariant set such that a dynamic gain scheduling control can be designed which will then be used to design a state feedback control to improve the dynamic performance of the elliptical orbit rendezvous under input saturation.

42
43
44
45
46
47
48
49
50
51
52
53

The main contributions of this paper are stated as follows: (i) Since T-H equations can be transformed into linear periodic system, the periodicity of the system can be used to design the required discrete gain scheduling control. Note that the discrete parameters of discrete gain scheduling control approach can preserve the periodicity of the solution of the periodic Riccati equation. (ii) Different from the discrete gain scheduling control design for the time-invariant H-C-W equations under input saturation, this paper constructs new time-varying elliptic sets not indirectly obtained from the level set of the Lyapunov function. With these new time-varying elliptic sets, some novel time-invariant elliptic invariant sets are constructed through the use of the rotation (reflection) transformation technique. These time-invariant elliptic invariant sets are then used to determine the switching points of the discrete gain scheduling control. These contributions are practically important and technically rather interesting. (iii) Compared with the static gain scheduling control approach, the discrete gain scheduling control approach can much improve the dynamic performance of the system under input saturation.

54
55
56
57
58
59

The rest of this paper is organized as follows. In Section 2, T-H equations are transformed into linear periodic system, and the spacecraft rendezvous problem is formulated. In Section 3, some preliminary results are presented. On this basis, the main results are presented in Section 4, which include the construction of invariant sets and the

design of the discrete gain scheduling control for accomplishing the rendezvous mission of the spacecraft. In Section 5, an illustrative example is considered and solved, showing the effectiveness of the proposed method. Finally, some concluding remarks are made in Section 6.

2 | PROBLEM FORMULATION

The spacecraft rendezvous process is depicted in Figure 1 .

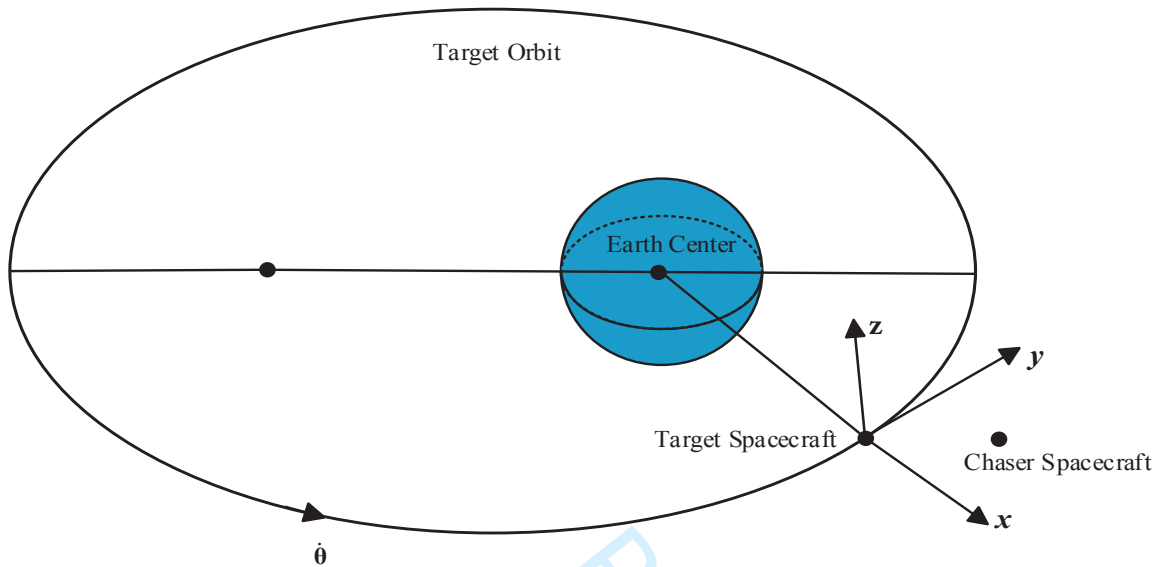


FIGURE 1 Spacecraft rendezvous process

Assume that the target spacecraft is moving along an eccentric orbit. The coordinate frame in our study is a rotating inertial coordinate, where the origin is at the mass center of the target spacecraft. The x -axis direction is from the earth center to the mass center of the target spacecraft, the y -axis is the moving direction of the target spacecraft on the eccentric orbit, and the z -axis is obtained by taking the cross product $x \times y$.

Let $e \in [0, 1)$ be the eccentricity of the eccentric orbit, and θ be the true anomaly. Then, $\dot{\theta} = k^2 \rho^2(\theta)$, where $\rho(\theta) = 1 + e \cos \theta$, and k is a constant. Suppose that the target spacecraft and chaser spacecraft are adjacent, i.e, the distance between the target spacecraft and the chaser spacecraft is much smaller than the distance between the mass center of the target spacecraft and the earth center. Then, the relative dynamic model is described by the following T-H equations:

$$\begin{bmatrix} \ddot{x}(t) \\ \ddot{y}(t) \\ \ddot{z}(t) \end{bmatrix} = \begin{bmatrix} 2k\dot{\theta}^{3/2}x(t) + 2\dot{\theta}\dot{y}(t) + \dot{\theta}^2x(t) + \ddot{\theta}y(t) \\ -k\dot{\theta}^{3/2}y(t) - 2\dot{\theta}\dot{x}(t) + \dot{\theta}^2y(t) - \ddot{\theta}x(t) \\ -k\dot{\theta}^{3/2}z(t) \end{bmatrix} + \text{sat}_\omega(u(t)) \quad (2.1)$$

where $[x(t), y(t), z(t)]$ represents the relative position, $[\dot{x}(t), \dot{y}(t), \dot{z}(t)]$ and $[\ddot{x}(t), \ddot{y}(t), \ddot{z}(t)]$ denote, respectively, the first order derivative and the second order derivative of $[x(t), y(t), z(t)]$ with respect to t , and $u(t) = [u_1(t), u_2(t), u_3(t)]^T$ is the acceleration vector of the chaser spacecraft, and $\text{sat}_\omega(u(t)) = [\text{sat}_\omega(u_1(t)), \text{sat}_\omega(u_2(t)), \text{sat}_\omega(u_3(t))]^T$, $\text{sat}_\omega(u_i(t))$ is defined in²⁶ as follows:

$$\text{sat}_\omega(u_i(t)) = \begin{cases} \omega, & u_i(t) > \omega \\ u_i(t), & |u_i(t)| \leq \omega, \quad i = 1, 2, 3 \\ -\omega, & u_i(t) < -\omega \end{cases}$$

Denote

$$\zeta(t) = [x(t), y(t), z(t), \dot{x}(t), \dot{y}(t), \dot{z}(t)]^T$$

Then, (2.1) can be reduced to the following first order linear system:

$$\dot{\zeta}(t) = \mathbb{A}(t)\zeta(t) + \mathbb{B}(t)\text{sat}_{\omega}(u(t)) \quad (2.2)$$

where

$$\mathbb{A}(t) = \begin{bmatrix} 0_3 & I_3 \\ \mathbb{A}_1(t) & \mathbb{A}_2(t) \end{bmatrix}, \mathbb{B}(t) = \begin{bmatrix} 0_3 \\ I_3 \end{bmatrix}$$

and

$$\mathbb{A}_1(t) = \begin{bmatrix} \dot{\theta}^2 + 2k\dot{\theta}^{3/2} & \ddot{\theta} & 0 \\ -\ddot{\theta} & \dot{\theta}^2 - k\dot{\theta}^{3/2} & 0 \\ 0 & 0 & -k\dot{\theta}^{3/2} \end{bmatrix}, \mathbb{A}_2(t) = \begin{bmatrix} 0 & 2\dot{\theta} & 0 \\ -2\dot{\theta} & 0 & 0 \\ 0 & 0 & 0 \end{bmatrix}$$

For simplicity purpose, the true anomaly θ is chosen as an independent variable, $\xi'(\theta)$ represents the derivative of $\xi(\theta)$ with respect to θ . Let $\mathbf{x}(\theta)$ and $\mathbf{u}(\theta)$ be, respectively, the new state vector and the control vector defined below:

$$\mathbf{x}(\theta) = T(\theta)\zeta(t), \mathbf{u}(\theta) = u(t) \quad (2.3)$$

where

$$T(\theta) = \begin{bmatrix} \rho(\theta)I_3 & 0 \\ -e \sin \theta I_3 & \frac{1}{k^2 \rho(\theta)} I_3 \end{bmatrix}$$

Then, system (2.2) can be transformed into the following linear 2π -periodic system:

$$\mathbf{x}'(\theta) = A(\theta)\mathbf{x}(\theta) + B(\theta)\text{sat}_{\omega}(\mathbf{u}(\theta)) \quad (2.4)$$

where $A(\theta)$, $B(\theta)$ are given, respectively, by

$$A(\theta) = \begin{bmatrix} 0_3 & I_3 \\ A_1(\theta) & A_2(\theta) \end{bmatrix}, B(\theta) = \frac{1}{k^4 \rho^3(\theta)} \begin{bmatrix} 0_3 \\ I_3 \end{bmatrix} \quad (2.5a)$$

$$A_1(\theta) = \begin{bmatrix} \frac{3}{\rho(\theta)} & 0 & 0 \\ 0 & 0 & 0 \\ 0 & 0 & -1 \end{bmatrix}, A_2(\theta) = \begin{bmatrix} 0 & 2 & 0 \\ -2 & 0 & 0 \\ 0 & 0 & 0 \end{bmatrix} \quad (2.5b)$$

Now, the spacecraft rendezvous control problem can be stated as follows: For system (2.4) under input saturation, find a discrete gain scheduling state feedback control in the form given below:

$$\begin{cases} \mathbf{u}(\theta, \varepsilon_{k-1}) = -F(\theta, \varepsilon_{k-1})\mathbf{x}(\theta), & \mathbf{x}(\theta) \in O(\Lambda_{\max}(\varepsilon_{k-1})) \setminus O(\Lambda_{\max}(\varepsilon_k)), \quad \theta \in [\Theta_{k-1}, \Theta_k), \quad k \in \mathbf{I}[1, N] \\ \mathbf{u}(\theta, \varepsilon_N) = -F(\theta, \varepsilon_N)\mathbf{x}(\theta), & \mathbf{x}(\theta) \in O(\Lambda_{\max}(\varepsilon_N)), \quad \theta \in [\Theta_N, +\infty) \end{cases} \quad (2.6)$$

such that the closed-loop spacecraft rendezvous system is asymptotically stable within any given bounded domain of attraction, where (2.6) is defined by (4.12).

3 | PRELIMINARIES

Lemma 1 (Zheng and Miao²⁷). Let $A \in R^{n \times n}$, $B \in R^{n \times n}$. Then, AB and BA have the same eigenvalues.

Lemma 2 (Harris and Martin²⁸). Let $A = (a_{ij}) \in R^{n \times n}$, and let $\lambda(A)$ be an eigenvalue of A . Then, $\lambda(A)$ varies continuously as a function of elements a_{ij} , $i, j \in \mathbf{I}[1, n]$.

Lemma 3 (Cauchy Interlace Theorem²⁹). Let A be an n -th order symmetric matrix, and let B be an m -th order principal sub-matrix of A . Suppose that the eigenvalues of A and B are listed as $\lambda_1 \leq \lambda_2 \leq \dots \leq \lambda_n$ and $\mu_1 \leq \mu_2 \leq \dots \leq \mu_m$, respectively. Then, $\lambda_k \leq \mu_{n-m+k} \leq \lambda_{n-m+k}$, $k \in \mathbf{I}[1, m]$.

Lemma 4 (Courant-Fisher min-max Theorem³⁰). Let $A \in R^{n \times n}$ be a real symmetric matrix, and let $\lambda_1 \leq \lambda_2 \leq \dots \leq \lambda_n$ be the n eigenvalues of A . Then,

$$\lambda_j = \min_{\dim(U)=j} \max_{x \in U, |x|=1} x^T A x, \quad j \in \mathbf{I}[1, n]$$

Lemma 5 (Zhou and Lin and Duan¹²). For system (2.4), where $A(\theta)$ and $B(\theta)$ are, respectively, defined by (2.5a) and (2.5b), consider the periodic Riccati equation

$$-P'(\theta) = A^T(\theta)P(\theta) + P(\theta)A(\theta) - P(\theta)B(\theta)R^{-1}(\theta)B^T(\theta)P(\theta) + \varepsilon P(\theta) \quad (3.1)$$

where $R(\theta) > 0$ is a given 2π -periodic matrix, and $\varepsilon \in (0, +\infty)$. Then,

(i) Equation (3.1) has a unique positive definite 2π -periodic solution $P(\theta, \varepsilon)$, and the following periodic Lyapunov equation

$$W'(\theta) = W(\theta)A^T(\theta, \varepsilon) + A(\theta, \varepsilon)W(\theta) - B(\theta)R^{-1}(\theta)B^T(\theta)$$

has a unique periodic positive definite solution $W(\theta, \varepsilon) = P^{-1}(\theta, \varepsilon)$.

(ii) Let $P(\theta, \varepsilon)$ be the 2π -periodic definite solution of (3.1). Then, the periodic linear state feedback control for system (2.4) is $u(\theta) = K(\theta)x(\theta)$, where $K(\theta) = -R^{-1}(\theta)B^T(\theta)P(\theta)$.

(iii) $P(\theta, \varepsilon)$ is monotonically increasing with respect to ε , and $\lim_{\varepsilon \rightarrow 0^+} P(\theta, \varepsilon) = 0, \forall \theta \in [\theta_0, +\infty)$.

4 | MAIN RESULTS

4.1 | Construction of invariant sets

For the positive definite 2π -periodic solution $P(\theta, \varepsilon)$ of (3.1), there exists an n -th order orthogonal matrix $Q(\theta, \varepsilon)$ such that

$$P(\theta, \varepsilon) = Q^T(\theta, \varepsilon)\Lambda(\theta, \varepsilon)Q(\theta, \varepsilon)$$

where

$$\Lambda(\theta, \varepsilon) = \text{diag}\{\lambda_1(\theta, \varepsilon), \dots, \lambda_n(\theta, \varepsilon)\}$$

and

$$\lambda_1(\theta, \varepsilon) \geq \lambda_2(\theta, \varepsilon) \geq \dots \geq \lambda_n(\theta, \varepsilon) > 0$$

From $\lim_{\varepsilon \rightarrow 0^+} P(\theta, \varepsilon) = 0$ in Lemma 5, it follows that

$$\lim_{\varepsilon \rightarrow 0^+} \sum_{j=1}^n \lambda_j(\theta, \varepsilon) = \lim_{\varepsilon \rightarrow 0^+} \text{tr}(P(\theta, \varepsilon)) = 0$$

This means that

$$\lim_{\varepsilon \rightarrow 0^+} \lambda_j(\theta, \varepsilon) = 0, j \in \mathbf{I}[1, n] \quad (4.1)$$

Note that $P(\theta, \varepsilon)$ is the positive definite solution of (3.1) with period 2π , i.e., $P(\theta + 2\pi, \varepsilon) = P(\theta, \varepsilon), \forall \theta \in [\theta_0, +\infty)$. Thus, $P(\theta, \varepsilon)$ is a differentiable function of θ , and it is also continuous on $[0, 2\pi]$. According to Lemma 2, $\lambda_j(\theta, \varepsilon), j \in \mathbf{I}[1, n]$, are continuous functions of elements of $P(\theta, \varepsilon)$. Since the interval for the continuous functions is closed and bounded, $\lambda_j(\theta, \varepsilon)$ for each $j \in \mathbf{I}[1, n]$ admits its maximum and minimum values on $[0, 2\pi]$, i.e.,

$$\hat{\lambda}_j(\varepsilon) = \max_{\theta \in [0, 2\pi]} \lambda_j(\theta, \varepsilon), \forall j \in \mathbf{I}[1, n] \quad (4.2)$$

From (4.1), (4.2) and $P(\theta, \varepsilon) > 0$, it is easy to deduce that $\hat{\lambda}_j(\varepsilon) > 0$, and

$$\lim_{\varepsilon \rightarrow 0^+} \hat{\lambda}_j(\varepsilon) = 0, \forall j \in \mathbf{I}[1, n] \quad (4.3)$$

Let

$$\hat{P}(\theta, \varepsilon) = Q^T(\theta, \varepsilon)\hat{\Lambda}(\varepsilon)Q(\theta, \varepsilon)$$

where

$$\hat{\Lambda}(\varepsilon) = \text{diag}\{\hat{\lambda}_1(\varepsilon), \dots, \hat{\lambda}_n(\varepsilon)\}$$

Then

$$0 < P(\theta, \varepsilon) \leq \hat{P}(\theta, \varepsilon) \quad (4.4)$$

Combining (4.3) with the boundedness of the orthogonal matrix $Q(\theta, \varepsilon)$, we have

$$\lim_{\varepsilon \rightarrow 0^+} \hat{P}(\theta, \varepsilon) = 0$$

Let

$$S_N = \{\varepsilon_0, \varepsilon_1, \dots, \varepsilon_N\}, \quad 0 < \varepsilon_0 < \varepsilon_1 < \dots < \varepsilon_N \quad (4.5)$$

and

$$P_{\max}(\theta, \varepsilon_k) = Q^\top(\theta, \varepsilon_k) \Lambda_{\max}(\varepsilon_k) Q(\theta, \varepsilon_k), \quad \Lambda_{\max}(\varepsilon_k) = \hat{\rho} \hat{\lambda}_1(\varepsilon_k) \hat{\Lambda}(\varepsilon_k) \quad (4.6)$$

where $\hat{\rho} = k^8(1+e)^6$. For $\varepsilon_k > 0$ and $k \in \mathbf{I}[0, N]$, define

$$O_\omega(P(\theta, \varepsilon_k)) = \{x : \hat{\rho} \hat{\lambda}_1(\varepsilon_k) x^\top P(\theta, \varepsilon_k) x \leq \omega^2\} \quad (4.7)$$

$$O_\omega(P_{\max}(\theta, \varepsilon_k)) = \{x : x^\top P_{\max}(\theta, \varepsilon_k) x \leq \omega^2\} \quad (4.8)$$

and

$$O_\omega(\Lambda_{\max}(\varepsilon_k)) = \{x : x^\top \Lambda_{\max}(\varepsilon_k) x \leq \omega^2\} \quad (4.9)$$

From (4.4), it is easy to see that

$$O_\omega(P_{\max}(\theta, \varepsilon_k)) \subseteq O_\omega(P(\theta, \varepsilon_k)) \quad (4.10)$$

When $\det(Q(\theta, \varepsilon_k)) = 1$, each element of A on the boundary of $O_\omega(P_{\max}(\theta, \varepsilon_k))$ is rotated to be A' on the boundary of $O_\omega(\Lambda_{\max}(\varepsilon_k))$. When $\det(Q(\theta, \varepsilon_k)) = -1$, each element of A on the boundary of $O_\omega(P_{\max}(\theta, \varepsilon_k))$ is first rotated to be A' , and then reflected to be A'' on the boundary of $O_\omega(\Lambda_{\max}(\varepsilon_k))$. From the two cases discussed above, it is clear that $O_\omega(P_{\max}(\theta, \varepsilon_k))$ can be transformed into $O_\omega(\Lambda_{\max}(\varepsilon_k))$, i.e., each element of the two sets $O_\omega(P_{\max}(\theta, \varepsilon_k))$ and $O_\omega(\Lambda_{\max}(\varepsilon_k))$ has a one-to-one corresponding relationship. The orthogonal transformation process can be described as shown in Figure 2.

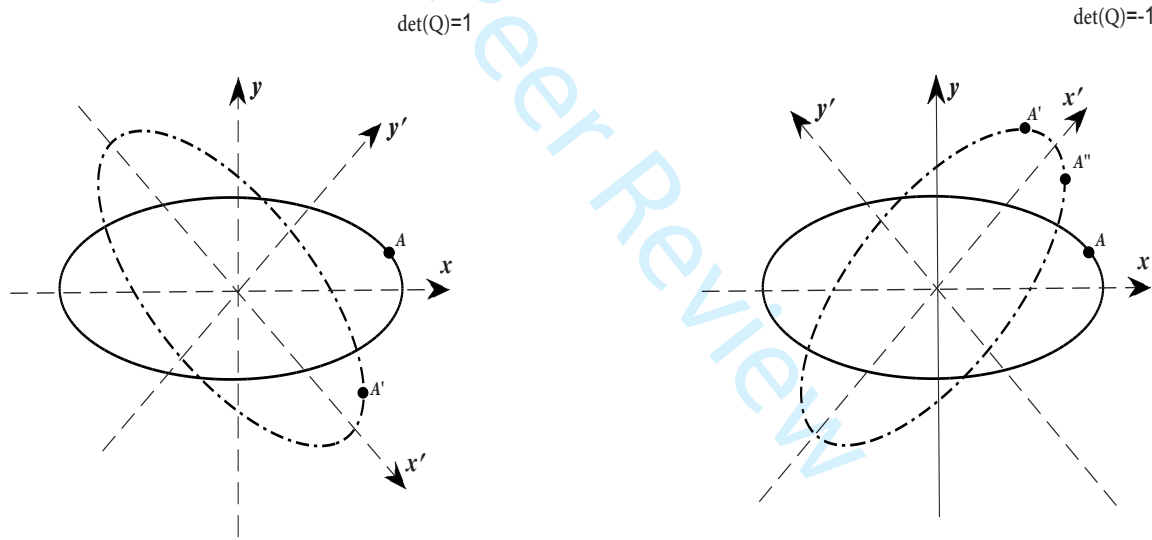


FIGURE 2 Orthogonal transformation process

For a given $\theta \in [0, 2\pi]$, $P(\theta, \varepsilon)$ is monotonically increasing with respect to ε , meaning that

$$P(\theta, \varepsilon_{k-1}) < P(\theta, \varepsilon_k), \quad k \in \mathbf{I}[1, N] \quad (4.11)$$

According to Lemma 4, it follows that

$$\begin{aligned} \lambda_j(\theta, \varepsilon_{k-1}) &= \min_{\dim(U)=j} \max_{x \in U, |x|=1} x^\top P(\theta, \varepsilon_{k-1}) x \\ &< \min_{\dim(U)=j} \max_{x \in U, |x|=1} x^\top P(\theta, \varepsilon_k) x \\ &= \lambda_j(\theta, \varepsilon_k), \quad k \in \mathbf{I}[1, N], \quad j \in \mathbf{I}[1, n] \end{aligned}$$

This, together with (4.2), yields

$$\hat{\lambda}_j(\varepsilon_{k-1}) < \hat{\lambda}_j(\varepsilon_k), \quad k \in \mathbf{I}[1, N], \quad j \in \mathbf{I}[1, n]$$

It is clear that

$$\Lambda_{\max}(\varepsilon_{k-1}) < \Lambda_{\max}(\varepsilon_k), \quad k \in \mathbf{I}[1, N]$$

Thus, the corresponding ellipsoids $O_\omega(\Lambda_{\max}(\theta, \varepsilon_k))$, $k \in \mathbf{I}[0, N]$, defined above are nested, i.e.,

$$O_\omega(\Lambda_{\max}(\varepsilon_0)) \supset O_\omega(\Lambda_{\max}(\varepsilon_1)) \supset \cdots \supset O_\omega(\Lambda_{\max}(\varepsilon_{N-1})) \supset O_\omega(\Lambda_{\max}(\varepsilon_N))$$

According to $O_\omega(\Lambda_{\max}(\varepsilon_k))$, $k \in \mathbf{I}[0, N]$, the switching points of the discrete gain scheduling control are determined as follows: For any initial state $\mathbf{x}(\theta_0)$, it follows from (iii) of Lemma 5 there exists an $\varepsilon_0 > 0$ such that

$$\mathbf{x}^\top(\theta_0)P_{\max}(\theta_0, \varepsilon_0)\mathbf{x}(\theta_0) = \omega^2$$

This, together with (4.6), yields

$$\mathbf{y}^\top(\theta_0)\Lambda_{\max}(\varepsilon_0)\mathbf{y}(\theta_0) = \omega^2$$

where $\mathbf{y}(\theta_0) = Q(\theta_0, \varepsilon_0)\mathbf{x}(\theta_0)$, which lies on the boundary of the ellipsoid $O_\omega(\Lambda_{\max}(\varepsilon_0))$. Since the ellipsoidal set $O_\omega(\Lambda_{\max}(\varepsilon_0))$ is invariant and the Lyapunov function is decreasing, it follows that the vector $Q(\theta, \varepsilon_0)\mathbf{x}(\theta)$ will stay inside the ellipsoid $O_\omega(\Lambda_{\max}(\varepsilon_0))$ for $\theta \geq \theta_0$, and it will arrive on the boundary of the ellipsoid $O_\omega(Q(\theta_1, \varepsilon_0)P_{\max}(\theta_1, \varepsilon_1)Q^\top(\theta_1, \varepsilon_0))$ in a finite time $\theta_1 - \theta_0$, i.e.,

$$\mathbf{x}^\top(\theta_1)P_{\max}(\theta_1, \varepsilon_1)\mathbf{x}(\theta_1) = \omega^2$$

This, together with (4.6), yields

$$\mathbf{y}^\top(\theta_1)\Lambda_{\max}(\varepsilon_1)\mathbf{y}(\theta_1) = \omega^2$$

where $\mathbf{y}(\theta_1) = Q(\theta_1, \varepsilon_1)\mathbf{x}(\theta_1)$, which lies on the boundary of the ellipsoid $O_\omega(\Lambda_{\max}(\varepsilon_1))$. Similar to the above switching point θ_1 , the switching point θ_k can also be determined as follows: For a given ε_{k-1} , $k \in \mathbf{I}[1, N]$, the vector $Q(\theta_{k-1}, \varepsilon_{k-1})\mathbf{x}(\theta_{k-1})$ is on the boundary of the ellipsoid $O_\omega(\Lambda_{\max}(\varepsilon_{k-1}))$, i.e.,

$$\mathbf{x}^\top(\theta_{k-1})P_{\max}(\theta_{k-1}, \varepsilon_{k-1})\mathbf{x}(\theta_{k-1}) = \omega^2$$

According to the relationship (4.6) between $P_{\max}(\theta_{k-1}, \varepsilon_{k-1})$ and $\Lambda_{\max}(\varepsilon_{k-1})$, it follows that

$$\mathbf{y}^\top(\theta_{k-1})\Lambda_{\max}(\varepsilon_{k-1})\mathbf{y}(\theta_{k-1}) = \omega^2$$

where $\mathbf{y}(\theta_{k-1}) = Q(\theta_{k-1}, \varepsilon_{k-1})\mathbf{x}(\theta_{k-1})$, which lies on the boundary of the ellipsoid $O_\omega(\Lambda_{\max}(\varepsilon_{k-1}))$. Since the ellipsoidal set $O_\omega(\Lambda_{\max}(\varepsilon_{k-1}))$ is invariant and the Lyapunov function is decreasing, it follows that the vector $Q(\theta, \varepsilon_{k-1})\mathbf{x}(\theta)$ will stay inside the ellipsoid $O_\omega(\Lambda_{\max}(\varepsilon_{k-1}))$ for $\theta \geq \theta_{k-1}$, and it will arrive on the boundary of the ellipsoid $O_\omega(Q(\theta_k, \varepsilon_{k-1})P_{\max}(\theta_k, \varepsilon_k)Q^\top(\theta_k, \varepsilon_{k-1}))$ in a finite time $\theta_k - \theta_{k-1}$, i.e.,

$$\mathbf{x}^\top(\theta_k)P_{\max}(\theta_k, \varepsilon_k)\mathbf{x}(\theta_k) = \omega^2$$

This, together with (4.6), yields

$$\mathbf{y}^\top(\theta_k)\Lambda_{\max}(\varepsilon_k)\mathbf{y}(\theta_k) = \omega^2$$

where $\mathbf{y}(\theta_k) = Q(\theta_k, \varepsilon_k)\mathbf{x}(\theta_k)$, which lies on the boundary of the ellipsoid $O_\omega(\Lambda_{\max}(\varepsilon_k))$. From the above switching process, it can be seen that the state $Q(\theta_k, \varepsilon_k)\mathbf{x}(\theta_k)$ will gradually approach to the original as k increases. Therefore, if the vector $Q(\theta, \varepsilon_k)\mathbf{x}(\theta)$ is inside the ellipsoid $O_\omega(\Lambda_{\max}(\varepsilon_k))$ for $\theta \in (\theta_k, \theta_{k+1})$, then the convergence speed of $Q(\theta, \varepsilon_k)\mathbf{x}(\theta)$ will increase as k increases. Since $\|Q(\theta, \varepsilon_k)\mathbf{x}(\theta)\| = \|\mathbf{x}(\theta)\|$, the convergence speed of the state of the closed-loop system will increase as k increases. Thus, the dynamic performance of the closed-loop system can be enhanced by increasing the convergence speed of the state, which is the main virtue of the discrete gain scheduling control approach. The gain scheduling process discussed above can be intuitively described as in Figure 3, where the switching points $\mathbf{y}(\theta_k)$, $k \in \mathbf{I}[1, N]$, of the discrete gain scheduling control are determined through the use of Algorithm A in Remark 3 to be stated below.

Remark 1. For the time-invariant H-C-W equations with input saturation, some ellipsoidal sets can be obtained from the level set of the Lyapunov function, and they are time-invariant and inclusive (see References^{17,18,19,20,21,22}). However, for the time-varying T-H equations with input saturation, if some ellipsoidal sets (4.7) are constructed directly from the level set of the Lyapunov function, then these ellipsoidal sets are time-varying, and may not be inclusive. Thus, the determination of the switching points of the discrete gain scheduling controller from these ellipsoidal sets will not be possible. In order to overcome these difficulties, some novel ellipsoidal sets (4.8) are required to be constructed such that (4.10) is satisfied. Now, based on (4.8), we shall construct some time-invariant ellipsoidal

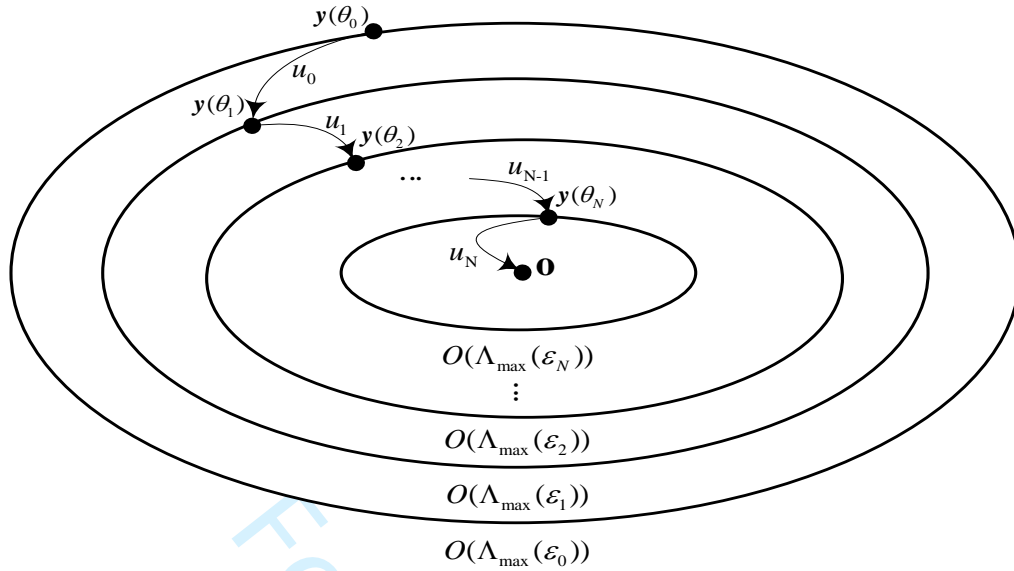


FIGURE 3 Switch points of control and state trajectories

invariant sets (4.9) through the novel application of the rotation (reflection) transformation. These time-invariant ellipsoidal invariant sets are defined by (4.9), and they can be used to determine the switching points of the discrete gain scheduling controller. Compared with the previous work, the construction of these time-invariant ellipsoidal invariant sets of this paper is practically important and technically nontrivial.

4.2 | Discrete gain scheduling control design

Theorem 1. Consider system (2.4), where $A(\theta)$ and $B(\theta)$ are, respectively, defined by (2.5a) and (2.5b). Let $P(\theta, \varepsilon)$ be a unique positive definite 2π -periodic solution of equation (3.1). Then, under the following discrete gain scheduling state feedback control

$$\begin{cases} \mathbf{u}_{k-1} = -R^{-1}(\theta)B^T(\theta)P(\theta, \varepsilon_{k-1})\mathbf{x}(\theta), & \mathbf{x}(\theta) \in \Xi(\varepsilon_{k-1}, \varepsilon_k), & \theta \in [\Theta_{k-1}, \Theta_k), & k \in \mathbf{I}[1, N] \\ \mathbf{u}_N = -R^{-1}(\theta)B^T(\theta)P(\theta, \varepsilon_N)\mathbf{x}(\theta), & \mathbf{x}(\theta) \in O_\omega(\Lambda_{\max}(\varepsilon_N)), & \theta \in [\Theta_N, +\infty) \end{cases} \quad (4.12)$$

the resulting input saturated closed-loop system (2.4) is asymptotically stable, and the domain of attraction of the closed-loop system is contained in a given arbitrary set Ω , where

$$\Xi(\varepsilon_{k-1}, \varepsilon_k) = O_\omega(\Lambda_{\max}(\varepsilon_{k-1})) \setminus O_\omega(\Lambda_{\max}(\varepsilon_k)), \quad k \in \mathbf{I}[1, N]$$

$$\Theta_{k-1} \leq \frac{1}{\varepsilon_{k-1}} \ln \left[\frac{\hat{\lambda}_1^2(\varepsilon_k)}{\hat{\rho}\hat{\lambda}_1(\varepsilon_{k-1})\hat{\lambda}_6(\varepsilon_{k-1})} \right], \quad k \in \mathbf{I}[1, N]$$

and

$$R(\theta) = \frac{1}{k^8 \rho^6(\theta)} I_3 \quad (4.13)$$

Proof : Let

$$P(\theta, \varepsilon) = \begin{bmatrix} P_{11}(\theta, \varepsilon) & P_{12}(\theta, \varepsilon) \\ P_{12}^T(\theta, \varepsilon) & P_{22}(\theta, \varepsilon) \end{bmatrix}$$

According to $B(\theta)$ in (2.5a) and $R(\theta)$ in (4.13), we have

$$R^{-1}(\theta)B^T(\theta)P(\theta, \varepsilon)B(\theta)R^{-1}(\theta) = k^8 \rho^6(\theta)P_{22}(\theta, \varepsilon)$$

From Lemma 3, it follows that

$$\lambda_{\max}(P_{22}(\theta, \varepsilon)) \leq \lambda_{\max}(P(\theta, \varepsilon))$$

which means that

$$\lambda_{\max}(R^{-1}(\theta)B^T(\theta)P(\theta, \varepsilon)B(\theta)R^{-1}(\theta)) \leq \lambda_{\max}(k^8 \rho^6(\theta)P(\theta, \varepsilon)) \quad (4.14)$$

Define:

$$\Omega_k := \left\{ \mathbf{x} : |R^{-1}(\theta)B^T(\theta)P(\theta, \varepsilon_k)\mathbf{x}| \leq \omega, \quad k \in \mathbf{I}[0, N] \right\}$$

By Lemma 1 and (4.14), we obtain

$$\begin{aligned} \|R^{-1}(\theta)B(\theta)P(\theta, \varepsilon_k)\mathbf{x}\|^2 &= \mathbf{x}^T P(\theta, \varepsilon_k)B(\theta)R^{-2}(\theta)B^T(\theta)P(\theta, \varepsilon_k)\mathbf{x} \\ &\leq \mathbf{x}^T P^{\frac{1}{2}}(\theta, \varepsilon_k)\lambda_{\max}(P^{1/2}(\theta, \varepsilon_k)B(\theta)R^{-2}(\theta)B^T(\theta)P^{1/2}(\theta, \varepsilon_k))P^{\frac{1}{2}}(\theta, \varepsilon_k)\mathbf{x} \\ &\leq \lambda_{\max}(R^{-1}(\theta)B^T(\theta)P(\theta, \varepsilon_k)B(\theta)R^{-1}(\theta))\mathbf{x}^T P(\theta, \varepsilon_k)\mathbf{x} \\ &\leq \lambda_{\max}(R^{-1}(\theta)B^T(\theta)\hat{P}(\theta, \varepsilon_k)B(\theta)R^{-1}(\theta))\mathbf{x}^T P(\theta, \varepsilon_k)\mathbf{x} \\ &\leq \lambda_{\max}(k^8 \rho^6(\theta)\hat{P}(\theta, \varepsilon_k))\mathbf{x}^T P(\theta, \varepsilon_k)\mathbf{x} \\ &\leq \hat{\rho}\hat{\lambda}_1(\varepsilon_k)\mathbf{x}^T \hat{P}(\theta, \varepsilon_k)\mathbf{x} \\ &= \mathbf{x}^T P_{\max}(\theta, \varepsilon_k)\mathbf{x} \\ &\leq \omega^2 \end{aligned} \quad (4.15)$$

By the definitions of Ω_k and $O_\omega(P_{\max}(\theta, \varepsilon_k))$, $k \in \mathbf{I}[0, N]$, it follows that $O_\omega(P_{\max}(\theta, \varepsilon_k)) \subseteq \Omega_k$, $\forall k \in \mathbf{I}[0, N]$. If $\mathbf{x} \in O_\omega(P_{\max}(\theta, \varepsilon_k))$, then, $\mathbf{x} \in \Omega_k$. This implies that the nonlinear saturation control $\text{sat}_\omega(\mathbf{u}(\theta))$ of (2.4) can be simplified as the piecewise linear control given by (4.12). Furthermore $\|\mathbf{u}\|_\infty \leq \omega$.

Choose the following Lyapunov functional

$$V_{k-1}(\mathbf{x}, \theta) = \hat{\lambda}_1(\varepsilon_{k-1})\mathbf{x}^T P(\theta, \varepsilon_{k-1})\mathbf{x}$$

Then,

$$\begin{aligned} \frac{dV_{k-1}(\mathbf{x}, \theta)}{d\theta} &= \hat{\lambda}_1(\varepsilon_{k-1})(\mathbf{x}')^T P(\theta, \varepsilon_{k-1})\mathbf{x} + \hat{\lambda}_1(\varepsilon_{k-1})\mathbf{x}^T P(\theta, \varepsilon_{k-1})\mathbf{x}' \\ &\quad + \hat{\lambda}_1(\varepsilon_{k-1})\mathbf{x}^T \frac{\partial P(\theta, \varepsilon)}{\partial \theta} \mathbf{x} \\ &= \hat{\lambda}_1(\varepsilon_{k-1})\mathbf{x}^T [A(\theta) - B(\theta)R^{-1}(\theta)B^T(\theta)P(\theta, \varepsilon_{k-1})]^T P(\theta, \varepsilon_{k-1})\mathbf{x} \\ &\quad + \hat{\lambda}_1(\varepsilon_{k-1})\mathbf{x}^T P(\theta, \varepsilon_{k-1})[A(\theta) - B(\theta)R^{-1}(\theta)B^T(\theta)P(\theta, \varepsilon_{k-1})]\mathbf{x} \\ &\quad + \hat{\lambda}_1(\varepsilon_{k-1})\mathbf{x}^T [-A^T(\theta)P(\theta, \varepsilon_{k-1}) - P(\theta, \varepsilon_{k-1})A(\theta) - \varepsilon_{k-1}P(\theta, \varepsilon_{k-1})]\mathbf{x} \\ &\quad + \hat{\lambda}_1(\varepsilon_{k-1})\mathbf{x}^T P(\theta, \varepsilon_{k-1})B(\theta)R^{-1}(\theta)B^T(\theta)P(\theta, \varepsilon_{k-1})\mathbf{x} \\ &< -\varepsilon_{k-1}\hat{\lambda}_1(\varepsilon_{k-1})\mathbf{x}^T P(\theta, \varepsilon_{k-1})\mathbf{x} \\ &= -\varepsilon_{k-1}V_{k-1}(\mathbf{x}, \theta) \end{aligned} \quad (4.16)$$

From (4.16), it follows that

$$\frac{dV_{k-1}(\mathbf{x}, \theta)}{d\theta} < 0, \quad \mathbf{x} \neq 0$$

and

$$\frac{dV_{k-1}(\mathbf{x}, \theta)}{d\theta} < -\varepsilon_{k-1}V_{k-1}(\mathbf{x}, \theta)$$

i.e.,

$$\frac{d \ln(V_{k-1}(\mathbf{x}, \theta))}{d\theta} < -\varepsilon_{k-1}, \quad \mathbf{x} \neq 0 \quad (4.17)$$

For $\theta \in [\theta_{k-1}, \theta_k)$, taking the integration of both sides of (4.17) from θ_{k-1} to θ , we obtain

$$V_{k-1}(\mathbf{x}(\theta), \theta) \leq V_{k-1}(\mathbf{x}(\theta_{k-1}), \theta_{k-1})e^{-\varepsilon_{k-1}(\theta - \theta_{k-1})}$$

This, together with (4.4), yields

$$\|\mathbf{x}(\theta)\| \leq \begin{cases} \alpha_{k-1}^{\frac{1}{2}} e^{-\frac{\varepsilon_{k-1}}{2}(\theta - \theta_{k-1})} \|\mathbf{x}(\theta_{k-1})\|, & \theta \in [\theta_{k-1}, \theta_k) \\ \alpha_N^{\frac{1}{2}} e^{-\frac{\varepsilon_N}{2}(\theta - \theta_N)} \|\mathbf{x}(\theta_N)\|, & \theta \in [\theta_N, +\infty) \end{cases}$$

where

$$\alpha_k = \frac{\hat{\lambda}_1(\varepsilon_k)}{\hat{\lambda}_6(\varepsilon_k)}, \quad k \in \mathbf{I}[1, N]$$

Let

$$\Theta_{k-1} = \theta_k - \theta_{k-1}$$

Then

$$\begin{aligned}
e^{-\varepsilon_{k-1}\Theta_{k-1}}\omega^2 &= e^{-\varepsilon_{k-1}\Theta_{k-1}}\mathbf{y}^\top(\theta_{k-1})\Lambda_{\max}(\varepsilon_{k-1})\mathbf{y}(\theta_{k-1}) \\
&= e^{-\varepsilon_{k-1}\Theta_{k-1}}\mathbf{x}^\top(\theta_{k-1})P_{\max}(\theta_{k-1}, \varepsilon_{k-1})\mathbf{x}(\theta_{k-1}) \\
&\geq \hat{\rho}e^{-\varepsilon_{k-1}\Theta_{k-1}}\hat{\lambda}_1(\varepsilon_{k-1})\mathbf{x}^\top(\theta_{k-1})P(\theta_{k-1}, \varepsilon_{k-1})\mathbf{x}(\theta_{k-1}) \\
&= \hat{\rho}e^{-\varepsilon_{k-1}\Theta_{k-1}}V_{k-1}[\mathbf{x}(\theta_{k-1}), \theta_{k-1}] \\
&\geq \hat{\rho}V_{k-1}[\mathbf{x}(\theta_k), \theta_k] \\
&= \hat{\rho}\hat{\lambda}_1(\varepsilon_{k-1})\mathbf{x}^\top(\theta_k)P(\theta_k, \varepsilon_{k-1})\mathbf{x}(\theta_k) \\
&= \hat{\rho}\hat{\lambda}_1(\varepsilon_{k-1})[Q(\theta_k, \varepsilon_{k-1})\mathbf{x}(\theta_k)]^\top\Lambda(\theta_k, \varepsilon_{k-1})Q(\theta_k, \varepsilon_{k-1})\mathbf{x}(\theta_k) \\
&\geq \frac{\hat{\rho}\hat{\lambda}_1(\varepsilon_{k-1})\check{\lambda}_6(\varepsilon_{k-1})}{\hat{\lambda}_1(\varepsilon_k)}\mathbf{y}^\top(\theta_k)\Lambda_{\max}(\varepsilon_k)\mathbf{y}(\theta_k) \\
&= \frac{\hat{\rho}\hat{\lambda}_1(\varepsilon_{k-1})\check{\lambda}_6(\varepsilon_{k-1})}{\hat{\lambda}_1^2(\varepsilon_k)}\omega^2
\end{aligned}$$

Thus,

$$\Theta_{k-1} \leq \frac{1}{\varepsilon_{k-1}} \ln \left[\frac{\hat{\lambda}_1^2(\varepsilon_k)}{\hat{\rho}\hat{\lambda}_1(\varepsilon_{k-1})\check{\lambda}_6(\varepsilon_{k-1})} \right]$$

Remark 2. From the proof of Theorem 1, it can be seen that the discrete gain scheduling state feedback control (4.12) is applied to system (2.4) in the order of $u_0 \rightarrow u_1 \rightarrow u_2 \rightarrow \dots \rightarrow u_N$. The discrete parameters ε_k , $k \in \mathbf{I}[0, N]$, influence the convergence speed of the closed-loop system (2.4). With the increase of the discrete parameters, the convergence speed of the closed-loop spacecraft rendezvous system (2.4) becomes faster and faster. Thus, the dynamic performances of the closed-loop spacecraft rendezvous system (2.4) can be much improved under the discrete gain scheduling state feedback control. This will be verified by an illustrative example in Section 5.

Remark 3. Based on Theorem 1, we have the following algorithm, referred to as Algorithm A, for the construction of the discrete gain scheduling control.

Step 1. For a given initial state $x(\theta_0)$, the solution ε_0 of the nonlinear equation

$$[Q(\theta_0, \varepsilon)x(\theta_0)]^\top\Lambda_{\max}(\varepsilon)[Q(\theta_0, \varepsilon)x(\theta_0)] = \omega^2 \quad (4.18)$$

can be computed by the bisection method.

Step 2. Given the common ratio $\Delta\varepsilon$ between the discrete parameters ε_{k-1} and ε_k , $k \in \mathbf{I}[1, N]$, the discrete parameters of the gain scheduling control form a set $S_N = \{\varepsilon_k, k \in \mathbf{I}[0, N]\}$ in (4.5), where $\varepsilon_k = \varepsilon_0 \cdot \Delta\varepsilon^k$, $k \in \mathbf{I}[0, N]$, and $\Delta\varepsilon$ is usually chosen as a fixed constant.

Step 3. By u_{k-1} and the state $x(\theta)$ of system (2.4), determine θ_k , $k \in \mathbf{I}[1, N]$, through the computation of

$$[Q(\theta, \varepsilon_k)x(\theta)]^\top\Lambda_{\max}(\varepsilon_k)[Q(\theta, \varepsilon_k)x(\theta)] = \omega^2$$

Step 4. From Steps 2 and 3, the discrete gain scheduling state feedback control (4.12) in Theorem 1 can be designed.

5 | SIMULATION RESULTS

In this section, a practical example will be provided to show the effectiveness of the proposed approach.

Suppose that the target spacecraft is moving along the geostationary transfer orbit, and chaser spacecraft is in its neighborhood, i.e., the distance between the target spacecraft and the chaser spacecraft is much smaller than the distance from the mass center of the target spacecraft to the earth center (see Reference¹²). For clarity, the main parameter values for the numerical simulations are listed as follows: semimajor axis $a = 2.4616 \times 10^7$ m, eccentricity $e = 0.73074$, period $T = 38436$ s, constant $k = 2.267 \times 10^{-2} / \text{s}^{1/2}$.

For simulation purpose, suppose that the initial condition of the spacecraft rendezvous system (2.2) is

$$\zeta(t_0) = [12000, 14000, -12000, 1, -1, 1]^\top$$

This means that the relative position and the relative velocity of the chaser spacecraft are

$$[x(t_0), y(t_0), z(t_0)] = [12000 \text{ m}, 14000 \text{ m}, -12000 \text{ m}]$$

and

$$[\dot{x}(t_0), \dot{y}(t_0), \dot{z}(t_0)] = [1 \text{ m/s}, -1 \text{ m/s}, 1 \text{ m/s}]$$

respectively. Let the initial true anomaly at time t_0 be $\theta_0 = 0.1\pi$, from the linear invertible transform (2.3), it is easy to compute that the initial condition of system (2.4) is

$$\mathbf{x}(\theta_0) = [20340, 23730, -20340, -1562, -4309, 3858]^T \quad (5.1)$$

This, together with equation (4.18), yields the initial parameter value $\varepsilon_0 = 0.85$. For comparison purpose, let the parameter set (4.5) be

$$S_N = \{\varepsilon_0, \varepsilon_1, \dots, \varepsilon_N\}, \quad 0 < \varepsilon_0 < \varepsilon_1 < \dots < \varepsilon_N$$

where $\Delta\varepsilon = 1.06$, $\varepsilon_k = \varepsilon_0 \cdot \Delta\varepsilon^k$, $k \in \mathbf{I}[0, N]$, and $N = 0, 10$ and 30 . According to these parameter values, the different discrete gain scheduling controls (4.12) of system (2.4) can be designed through the application of Algorithm A in Remark 3. For the discrete gain scheduling controls corresponding to $N = 0$, $N = 10$ and $N = 30$, the state response signals of the closed-loop spacecraft rendezvous system are shown, respectively, in Figures 4 -9 , and the control input signals of the closed-loop spacecraft rendezvous system are as shown in Figures 10 -12 . From Figures 4 -9 and Figures 10 -12 , it can be seen that the closed-loop spacecraft rendezvous system (2.4) is asymptotically stable, and the control input signals of the closed-loop spacecraft rendezvous system satisfy the input saturation. This simulation results show that under the saturated discrete gain scheduling control, the rendezvous mission can be accomplished at around $\theta_f = 28.2618$ rad for $N = 0$, $\theta_f = 9.7452$ rad for $N = 10$ and $\theta_f = 2.6829$ rad for $N = 30$, respectively.

It is worth mentioning that the discrete gain scheduling control for $N = 0$ is actually a static state feedback control. Compared with the static state feedback control corresponding to $N = 0$, we see that the discrete gain scheduling control for $N = 10$ can be used to achieve the spacecraft rendezvous mission at around $\theta_f = 9.7452$ rad , saving over 18.5166 rad, the discrete gain scheduling control for $N = 30$ can be used to achieve the spacecraft rendezvous mission at around $\theta_f = 2.6829$ rad , saving over 25.5789 rad. This clearly shows the proposed discrete gain scheduling control approach can improve the dynamic performance of the system. In addition, Figures 10 -12 show that the proposed controller makes full use of the actuator capacity. However, the control inputs do not exceed the maximal allowable constraints during the entire rendezvous process. The simulation is carried out for three different cases: $N = 0$, $N = 10$ and $N = 30$. Their respective state trajectories of the closed-loop spacecraft rendezvous system (2.4) are recorded in Figure 13 . From these simulation results, it can be seen that as the value of N increases, the dynamic performance of the system will become better and better at the expense of the magnitude of the control input signal.

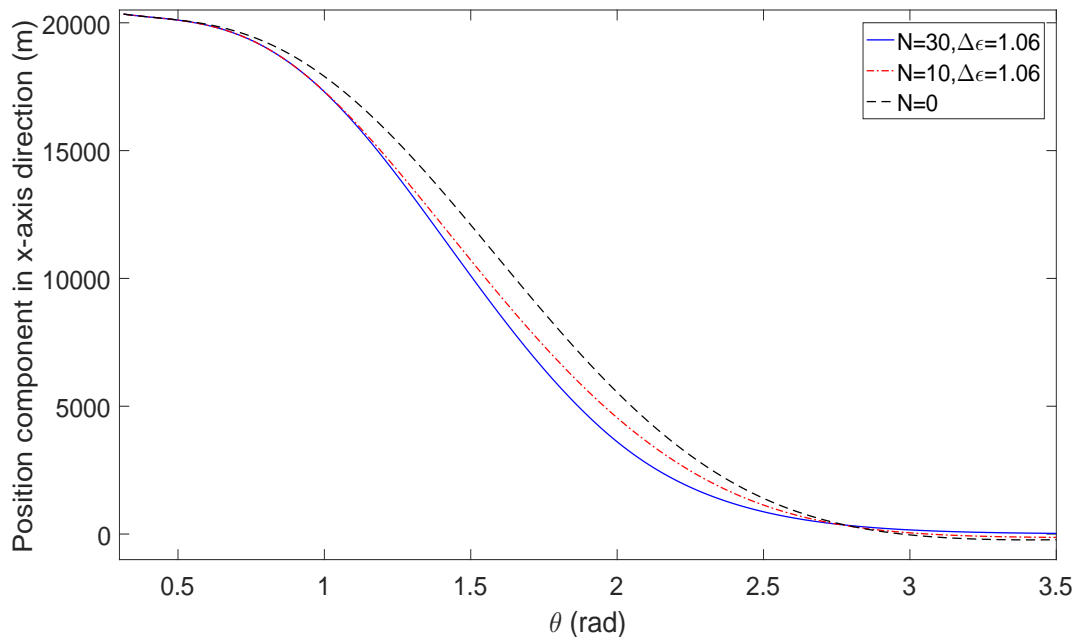


FIGURE 4 The position trajectories in x-axis direction with different switching points for $N = 0, 10, 30$

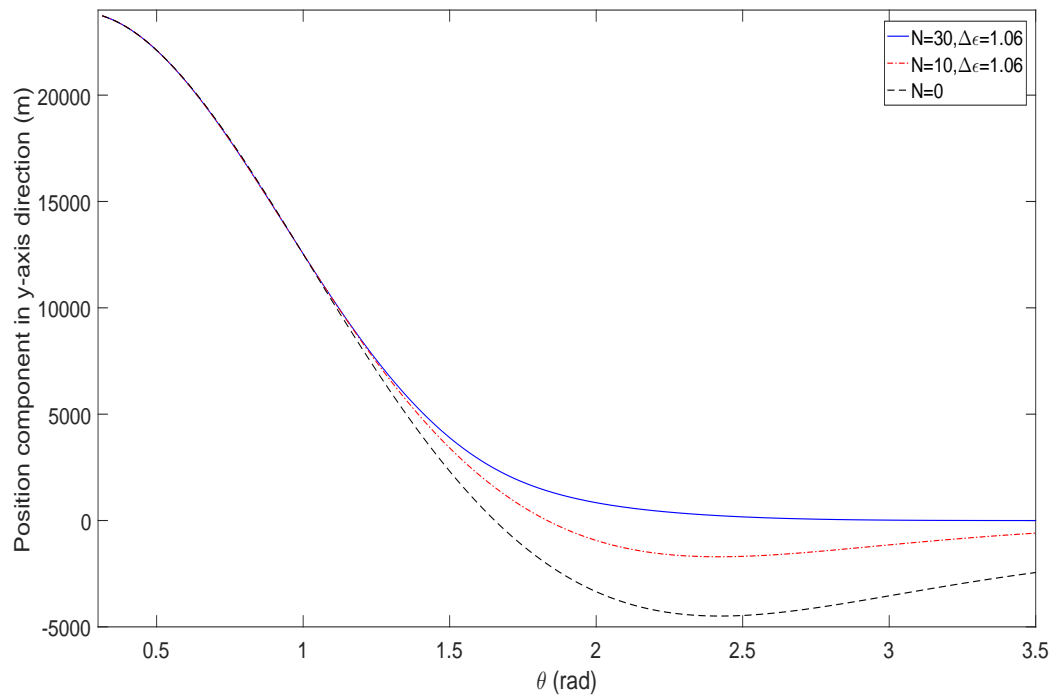


FIGURE 5 The position trajectories in y-axis direction with different switching points for $N = 0, 10, 30$

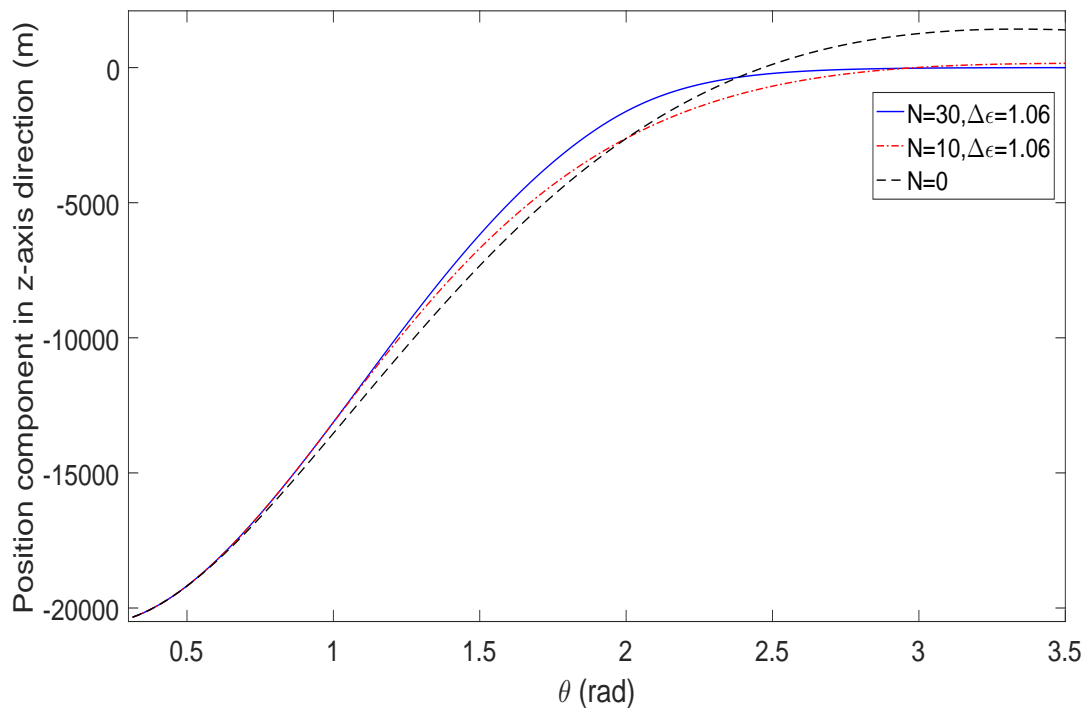


FIGURE 6 The position trajectories in z-axis direction with different switching points for $N = 0, 10, 30$

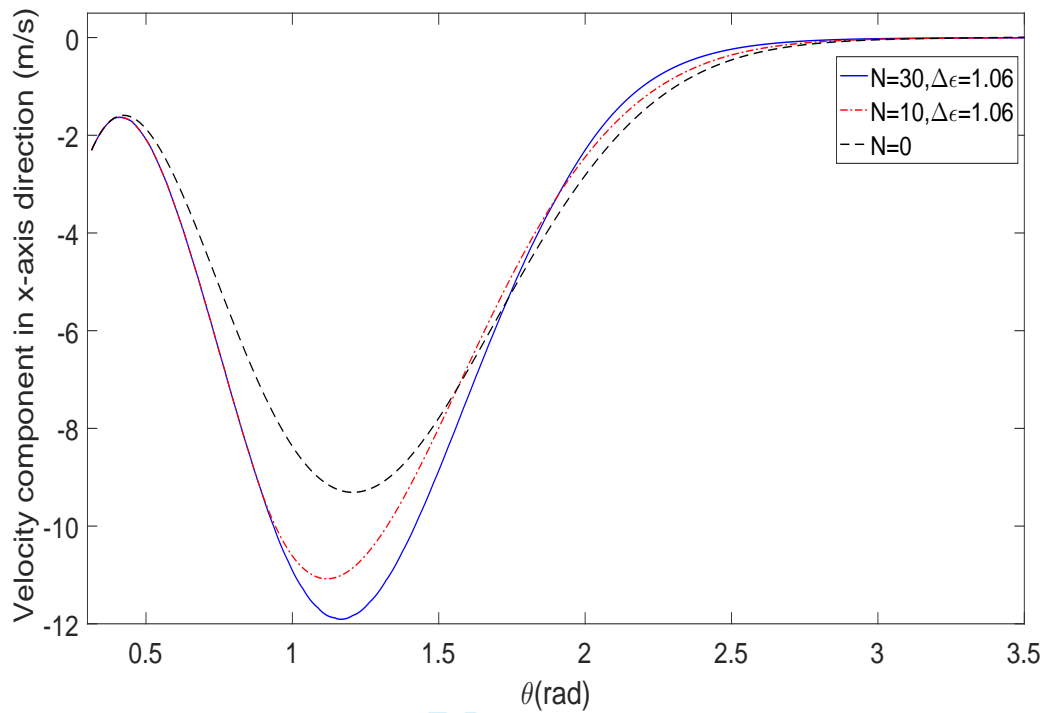


FIGURE 7 The velocity trajectories in x-axis direction with different switching points for $N = 0, 10, 30$

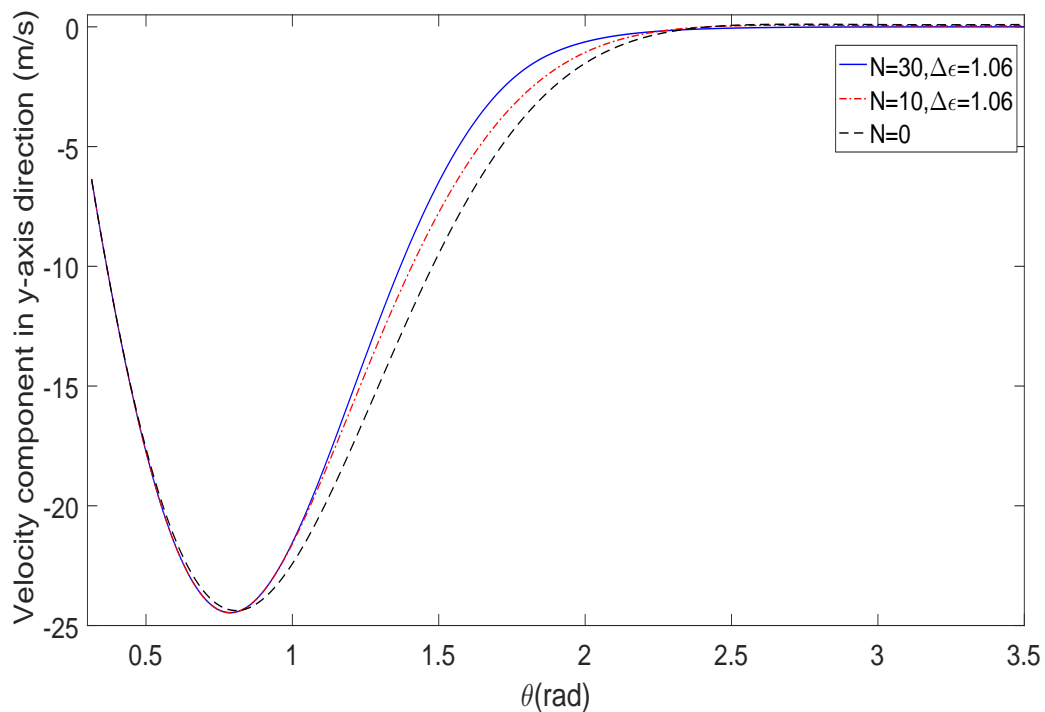


FIGURE 8 The velocity trajectories in y-axis direction with different switching points for $N = 0, 10, 30$

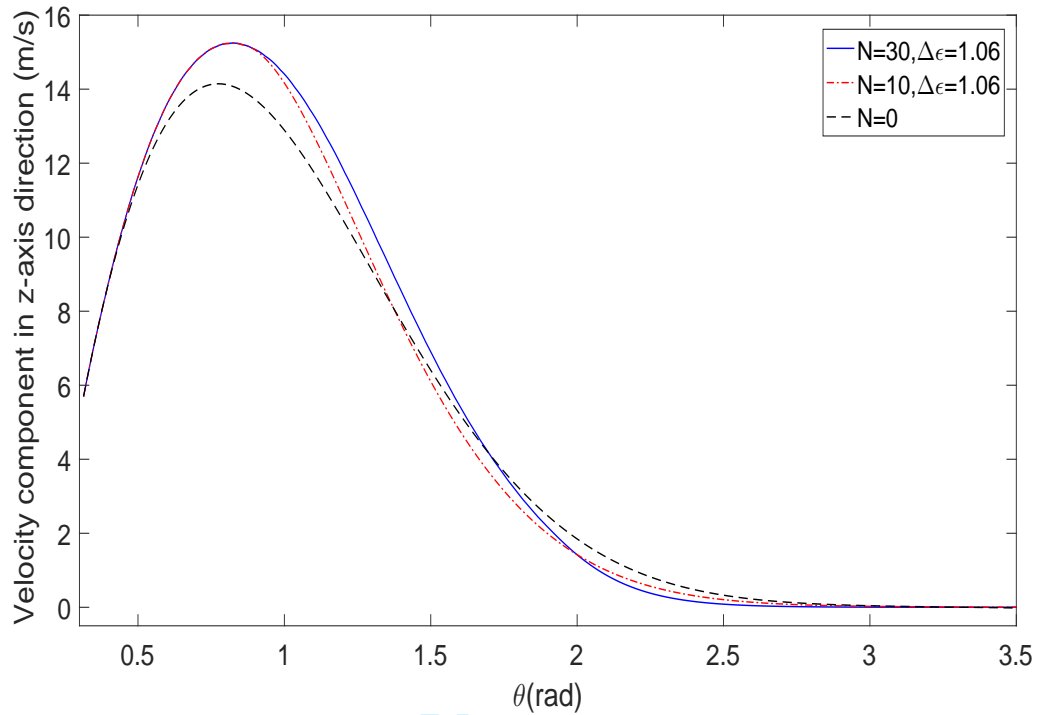


FIGURE 9 The velocity trajectories in z-axis direction with different switching points for $N = 0, 10, 30$

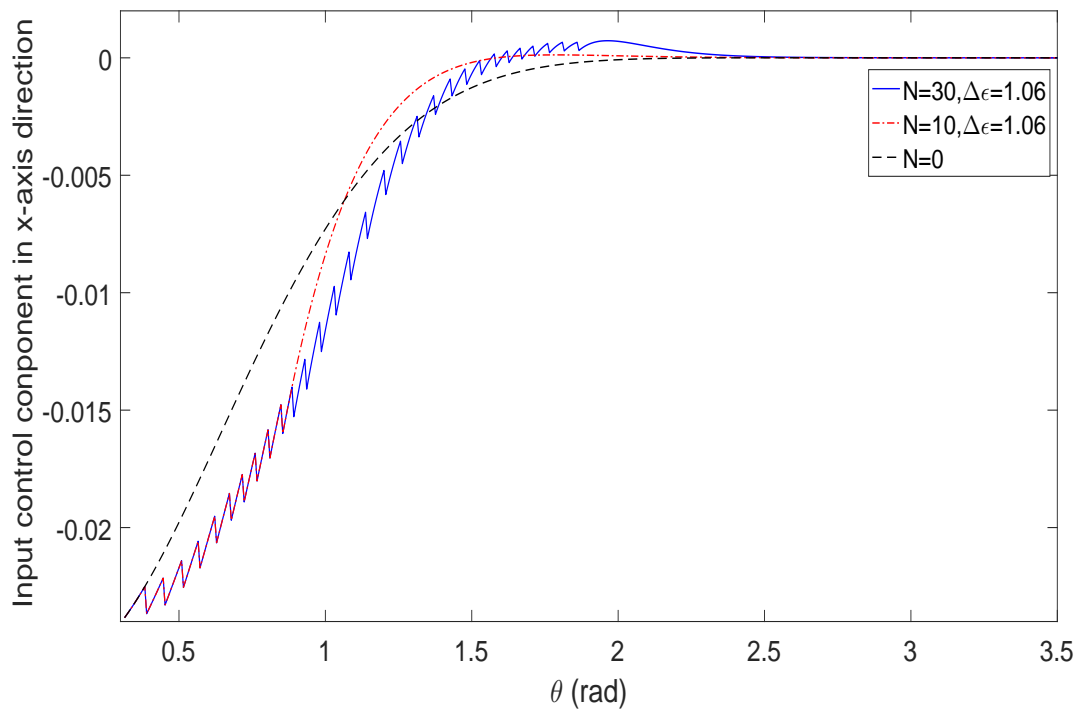


FIGURE 10 Control input signals in x-axis direction with different switching points for $N = 0, 10, 30$

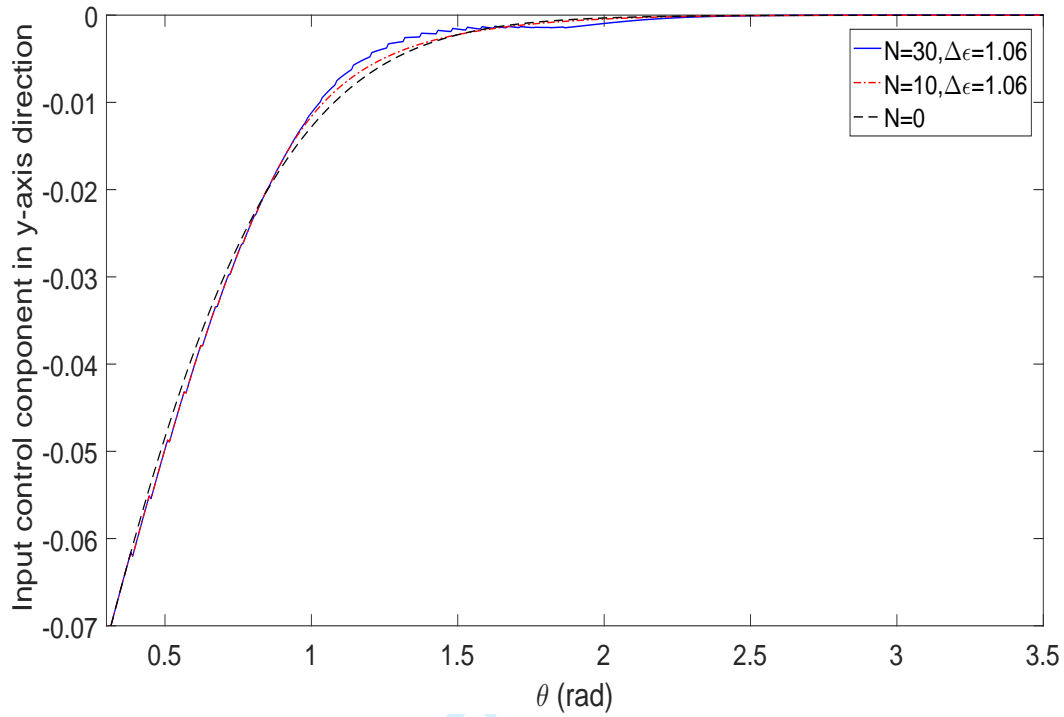


FIGURE 11 Control input signals in y-axis direction with different switching points for $N = 0, 10, 30$

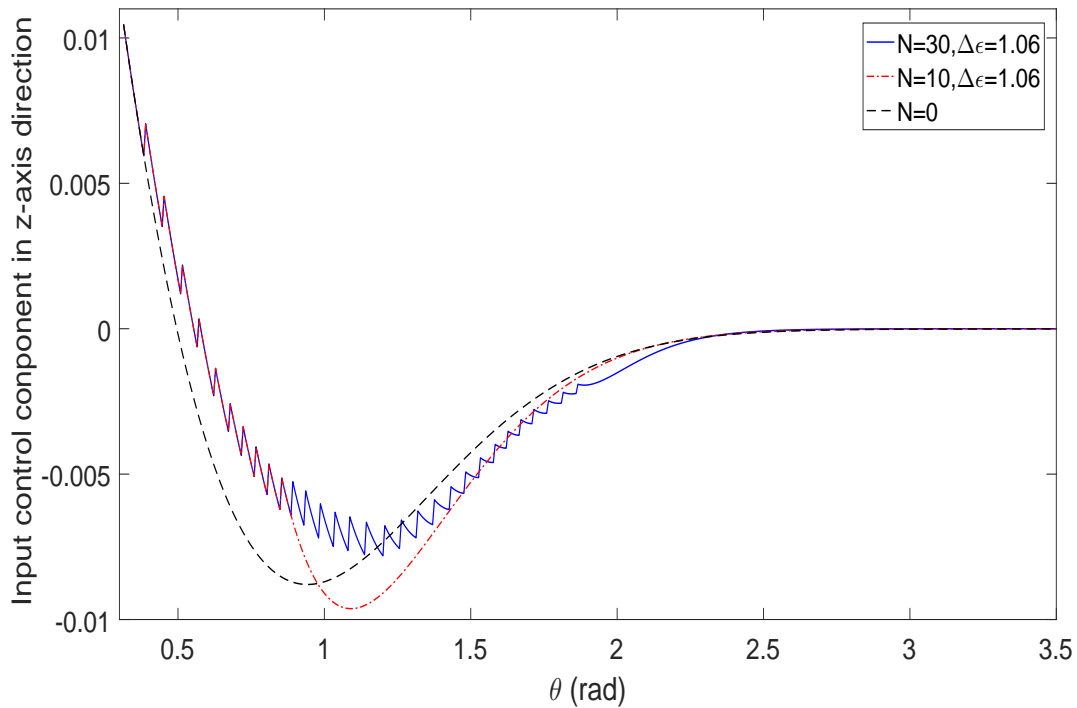


FIGURE 12 Control input signals in z-axis direction with different switching points for $N = 0, 10, 30$

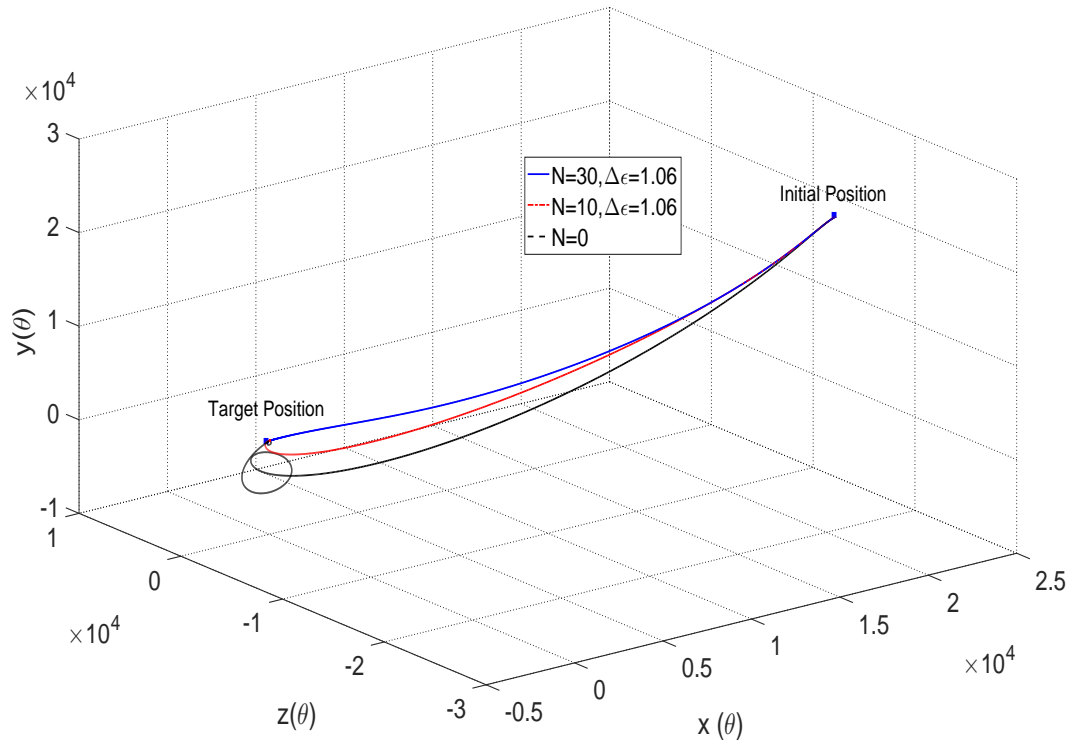


FIGURE 13 The trajectory with different switching points for $N = 0, 10, 30$

6 | CONCLUSIONS

In this paper, a discrete gain scheduling approach is used to design a state feedback control for an elliptical orbit spacecraft rendezvous system with actuator saturation, where the switching points of this approach are achieved through the construction of novel invariant sets. The main advantage of the proposed approach is that the dynamic performance of the spacecraft rendezvous can be much improved through adjusting the discrete parameters. Finally, simulation results show the effectiveness of the proposed control design method.

ACKNOWLEDGMENT

This work was partially supported by the Natural Science Foundation of Guangxi Province [grant number 2021GXNSFBA196080], the Humanities Social Sciences research Center of Guangxi [grant number LJGD202005], the National Natural Science Foundation of China [grant number 12101144], the Australian Research Council [grant number DP190103361], the Fundamental Research Grant Scheme of Malaysia [grant number FRGS/1/2021/STG06/SYUC/03/1] and the Innovation and Entrepreneurship Education Research Fund of Guangxi Normal University [grant numbers CXCYSZ2021009, CXCYSZ2021012].

CONFLICT OF INTEREST

The authors declared that they have no conflicts of interest to this work.

DATA AVAILABILITY STATEMENT

Data sharing is not applicable to this article as no datasets were generated or analyzed during the current study.

References

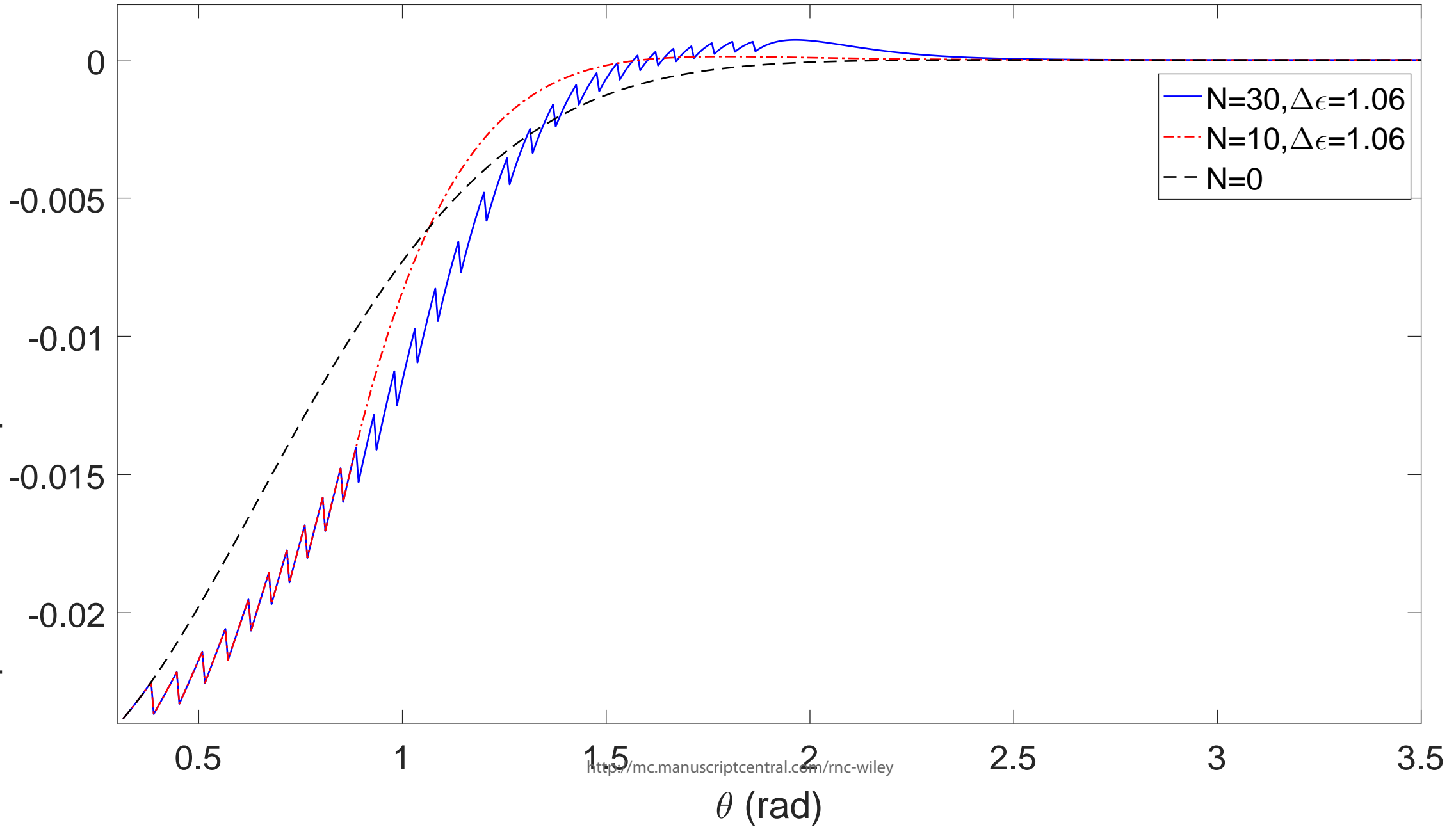
1. Clohessy WH, Wiltshire RS. Terminal guidance system for satellite rendezvous. *J Aerosp Sci.* 1960;27(9):653–658.
2. Carter TE. State transition matrices for terminal rendezvous studies: Brief survey and new example. *J Guid Control Dyn.* 1998;21(1):148–155.
3. Qi Y, Jia Y. Constant thrust fuel-optimal control for spacecraft rendezvous. *Adv Space Res.* 2012;49(7):1140–1150.
4. Yang X, Gao H. Robust reliable control for autonomous spacecraft rendezvous with limited-thrust. *Aerosp Sci Technol.* 2013;24(1):161–168.
5. Zhu Z, Xia Y, Fu M. Adaptive sliding mode control for attitude stabilization with actuator saturation. *IEEE Trans Ind Electron.* 2011;58(10):4898–4907.
6. Gao H, Yang X, Shi P. Multi-objective robust H_∞ control of spacecraft rendezvous. *IEEE Trans Control Syst Technol.* 2009;17(4):794–802.
7. Gao X, Teo KL, Duan G. Non-fragile robust H_∞ control for uncertain spacecraft rendezvous system with pole and input constraints. *Int J Control.* 2012;85(7):933–941.
8. Zhang K, Duan G. Robust H_∞ dynamic output feedback control for spacecraft rendezvous with poles and input constraint. *Int J Syst Sci.* 2017;48(5):1022–1034.
9. Li Z, Yu G, Zhang Q, Song S, Cui H. Adaptive sliding mode control for spacecraft rendezvous with unknown system parameters and input saturation. *IEEE Access.* 2021;9:67724–67733.
10. Namdari H, Allahverdizadeh F, Sharifi A. Robust composite nonlinear feedback control for spacecraft rendezvous systems under parameter uncertainty, external disturbance, and input saturation. *Proc IMechE, Part G: J Aerospace Engineering.* 2020;234(2):143–155.
11. Zhou B, Cui N, Duan G. Circular orbital rendezvous with actuator saturation and delay: a parametric Lyapunov equation approach. *IET Control Theory Appl.* 2012;6(9):1281–1287.
12. Zhou B, Lin Z, Duan G. Lyapunov differential equation approach to elliptical orbital rendezvous with constrained controls. *J Guid Control Dyn.* 2011;34(2):345–358.
13. Gao X, Teo KL, Duan G. An optimal control approach to spacecraft rendezvous on elliptical orbit. *Optim Control Appl Meth.* 2015;36(2):158–178.
14. Zhang K, Zhou B, Jiang H. Parametric Lyapunov equation based event-triggered and self-triggered control of input constrained linear systems. *Int J Robust Nonlinear Control.* 2020;30(16):6606–6626.
15. Zhou B. On semi-global stabilization of linear periodic systems with control magnitude and energy saturations. *J Franklin Inst.* 2015;352(5):2204–2228.
16. Wang Q, Zhou B, Duan G. Global stabilization of spacecraft rendezvous system subject to input saturation via gain scheduling. *Proc Chin Control Conf.* 2013;1436–1441.
17. Zhou B, Wang Q, Lin Z, Duan G. Gain scheduled control of linear systems subject to actuator saturation with application to spacecraft rendezvous. *IEEE Trans Control Syst Technol.* 2014;22(5):2031–2038.
18. Wang Q, Zhou B, Duan G. Discrete gain scheduled control of input saturated systems with applications in on-orbit rendezvous. *Acta Autom Sin.* 2014;40(2):208–218.

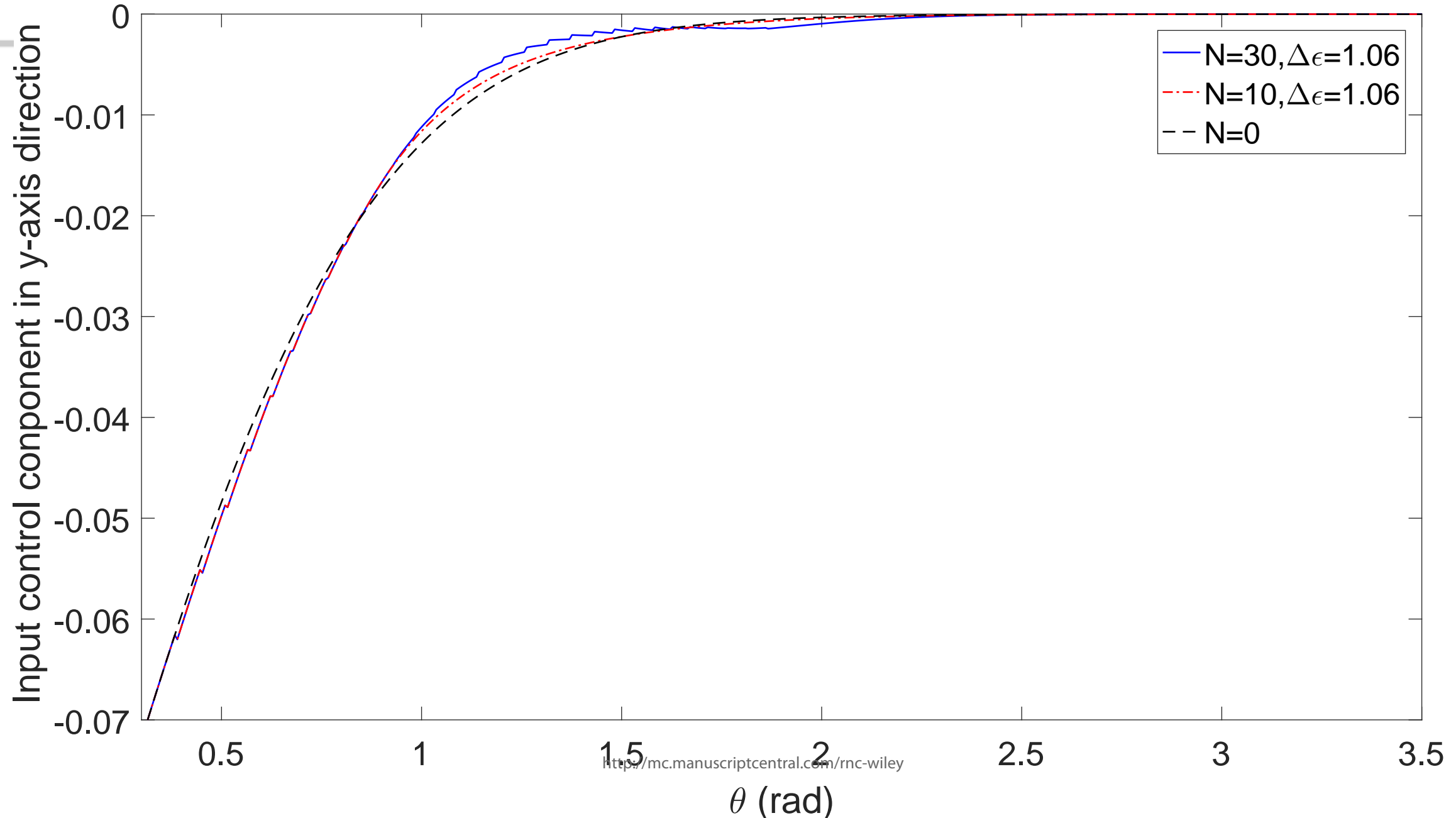
- 18 |
19. Wang Q, Zhou B, Wen C, Duan G. Output feedback gain scheduled control of actuator saturated linear systems with applications to the spacecraft rendezvous. *J Franklin Inst.* 2014;351(11):5015–5033.
 20. Wang Q, Xue A. Robust control for spacecraft rendezvous system with actuator unsymmetrical saturation: a gain scheduling approach. *Int J Control.* 2018;91(6):1241–1250.
 21. Huang Y, Jia Y. Output feedback robust H_∞ control for spacecraft rendezvous system subject to input saturation: a gain scheduled approach. *J Franklin Inst.* 2019;356(7):3899–3921.
 22. Zhang K, Zhou B, Jiang H, Duan G. Event-triggered and self-triggered gain scheduling control of input constrained systems with applications to the spacecraft rendezvous. *Int J Robust Nonlinear Control.* 2021;31(10):4629–4646.
 23. Hu T, Lin Z. *Control systems with actuator saturation: analysis and design.* Springer, Boston, MA; 2001.
 24. Fu J, Wu Q, Jiang C, Wang Y. Robust sliding mode positively invariant set control for a class of nonlinear continuous systems. *Acta Autom Sin.* 2011;37(11):1395–1401.
 25. Blanchini F. Set invariance in control. *Automatica.* 1999;35(11):1747–1767.
 26. Wang Q, Chen G, Yu H. Stability analysis and control synthesis for linear systems with non-symmetrical input saturation. *J Franklin Inst.* 2019;356(16):9565–9579.
 27. Zheng B, Miao S. Two new modified Gauss-Seidel methods for linear system with M -matrices. *J Comput Appl Math.* 2009;233(4):922–930.
 28. Harris G, Martin C. The roots of a polynomial vary continuously as a function of the coefficients. *Proc Amer Math Soc.* 1987;100(2):390–392.
 29. Hwang S. Cauchy's interlace theorem for eigenvalues of Hermitian matrices. *Amer Math Monthly.* 2004;111(2):157–159.
 30. Golub G, Van Loan C. *Matrix computations.* Johns Hopkins Studies in the Mathematical Sciences Johns Hopkins University Press, Baltimore, MD; third ed.1996.

How to cite this article: Gao X, He D, Teo KL, Wang J, Yang H, Discrete gain scheduling approach to elliptical orbit rendezvous system with actuator saturation, ******, 00 (2022) 1–16.

Author Manuscript

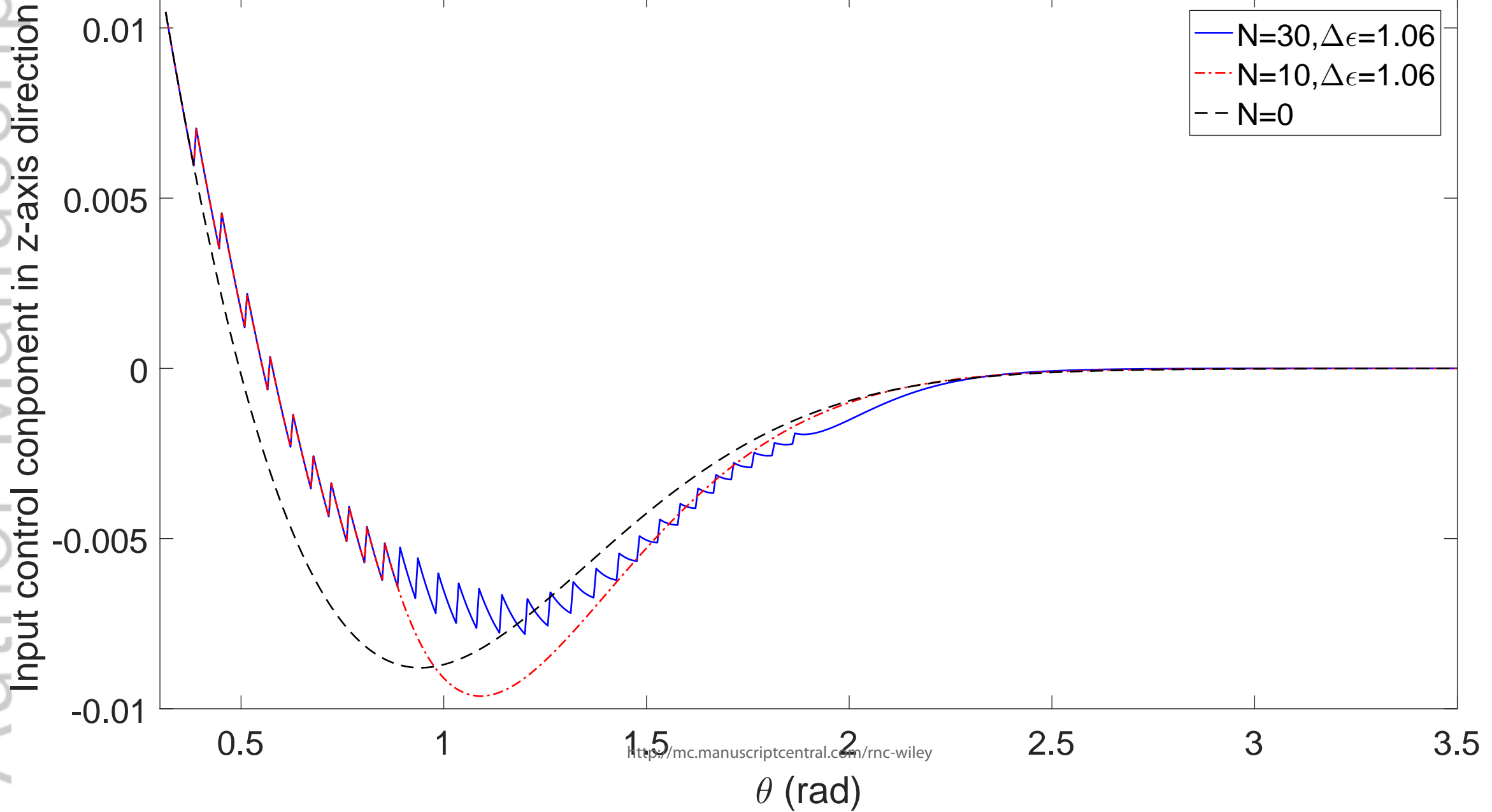
Input control component in x-axis direction

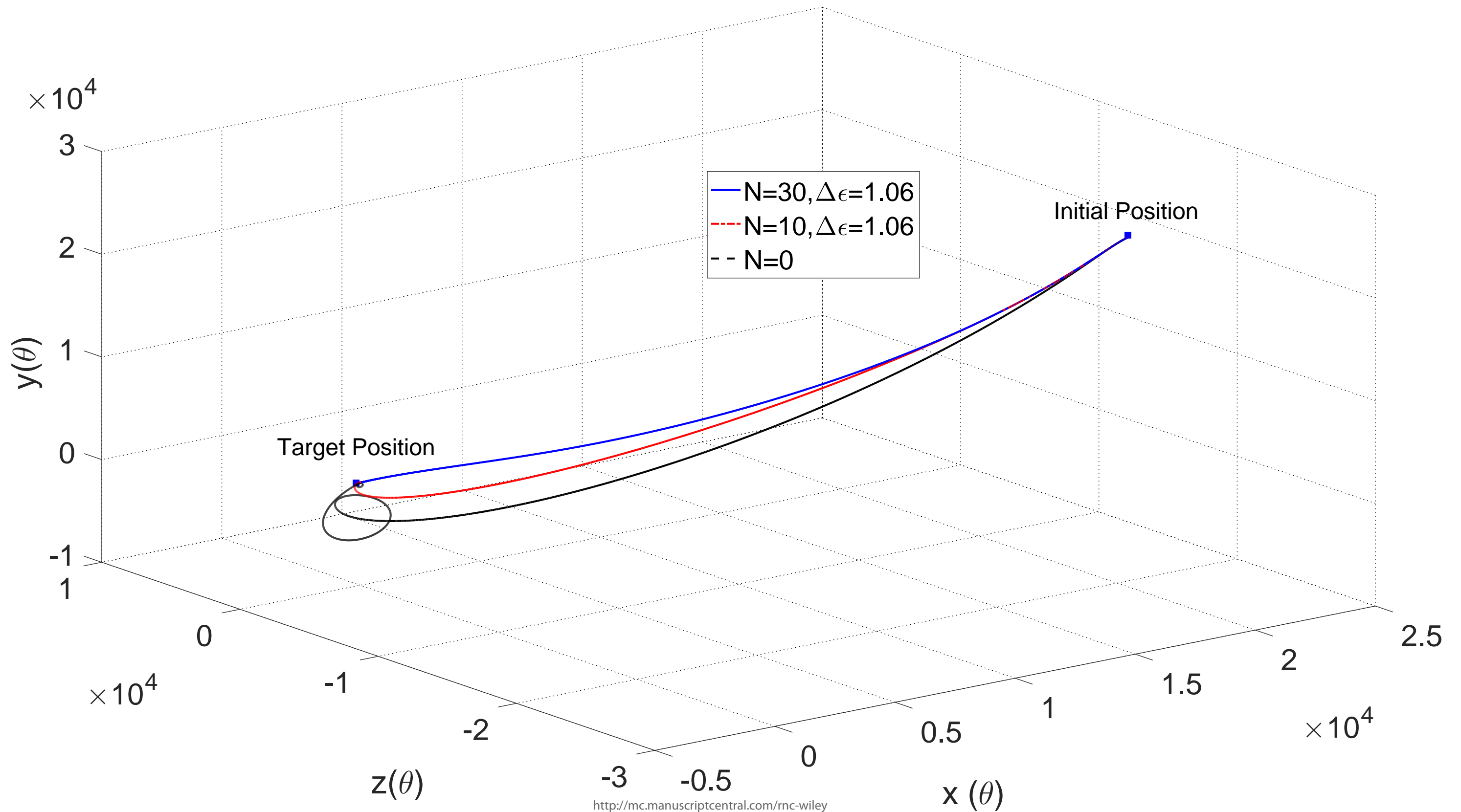




Author Manuscript

<http://mc.manuscriptcentral.com/rnc-wiley>

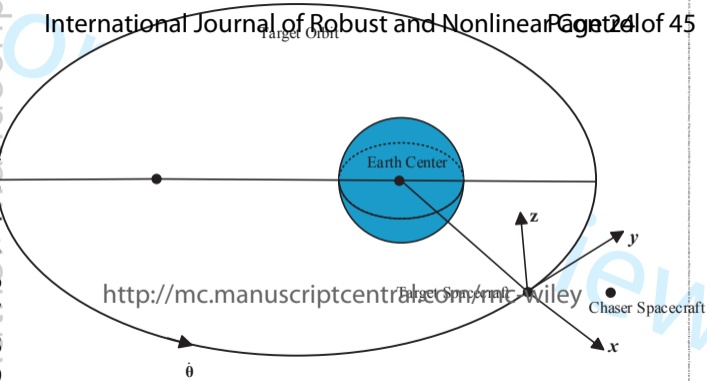




1
2
3
4
5
6
7
8
9
10
11
12
13
14
15
16
17
18
19
20
21
22
23
24
25
26
27
28
29
30
31
32
33
34
35
36
37
38
39
40
41
42
43
44
45
46
47
48
49
50
51
52
53
54
55

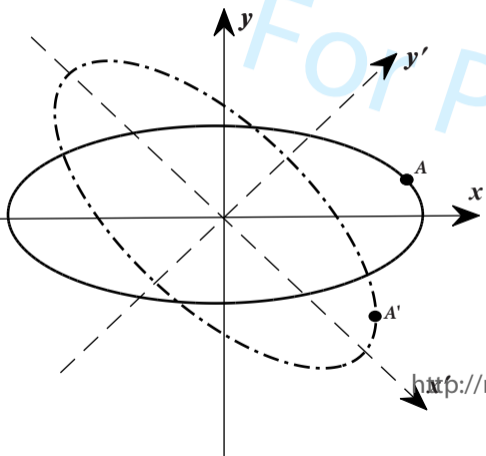
1091239, 2023, 3, Downloaded from https://onlinelibrary.wiley.com/doi/10.1002/rnc.6999 by Curtin University Library, Wiley Online Library on [08/04/2024]. See the Terms and Conditions (https://onlinelibrary.wiley.com/terms-and-conditions) on Wiley Online Library for rules of use; OA articles are governed by the applicable Creative Commons License

1
2
3
4
5
6
7
8
9

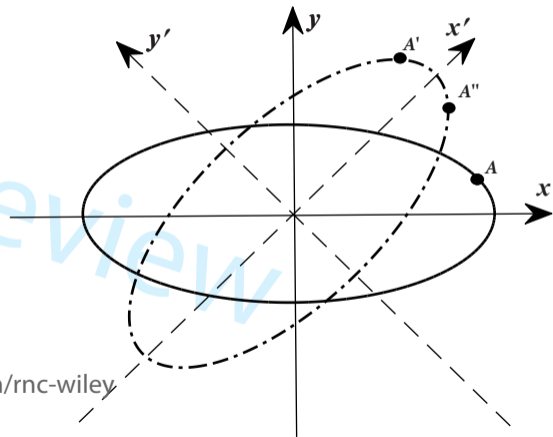


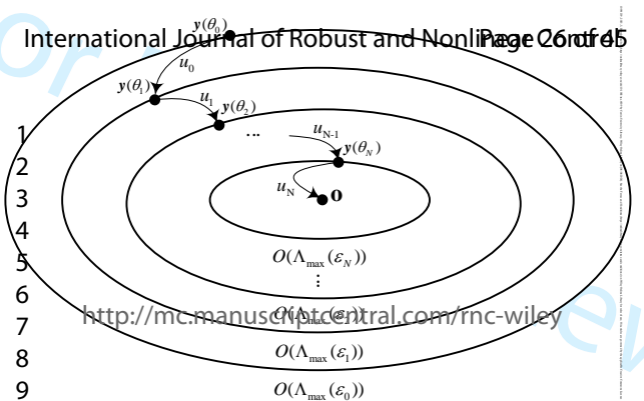
Manuscript received 12 October 2013; revised 12 October 2013; accepted 12 October 2013. This paper is published in the International Journal of Robust and Nonlinear Control, Vol. 24, No. 1, pp. 1-14, January 2014. © 2014 Taylor & Francis Ltd. DOI: 10.1080/17447591.2014.900000

1
2
3
4
5
6
7
8
9
10
11
12
13
14
15



<http://mc.manuscriptcentral.com/rnc-wiley>



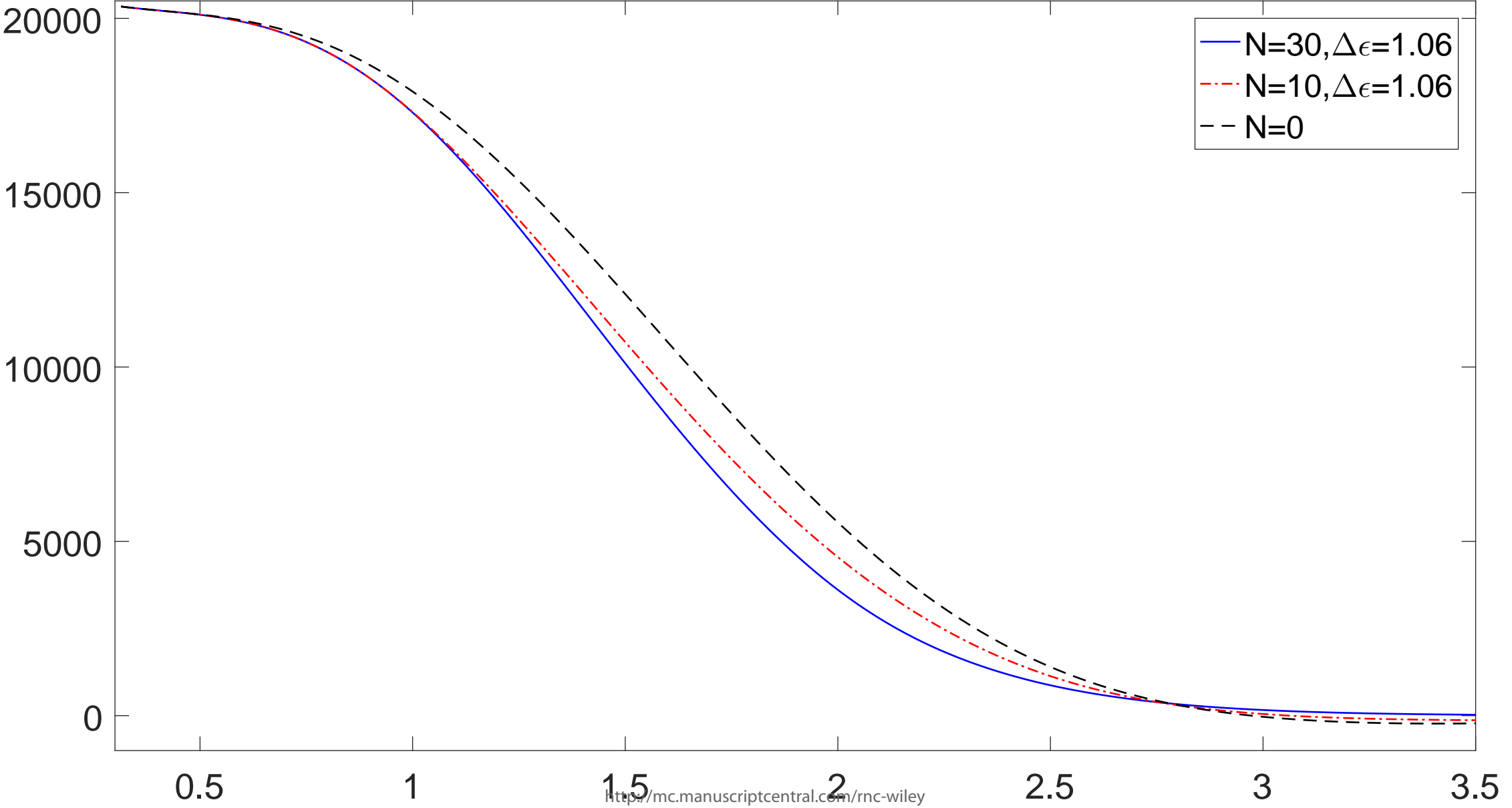


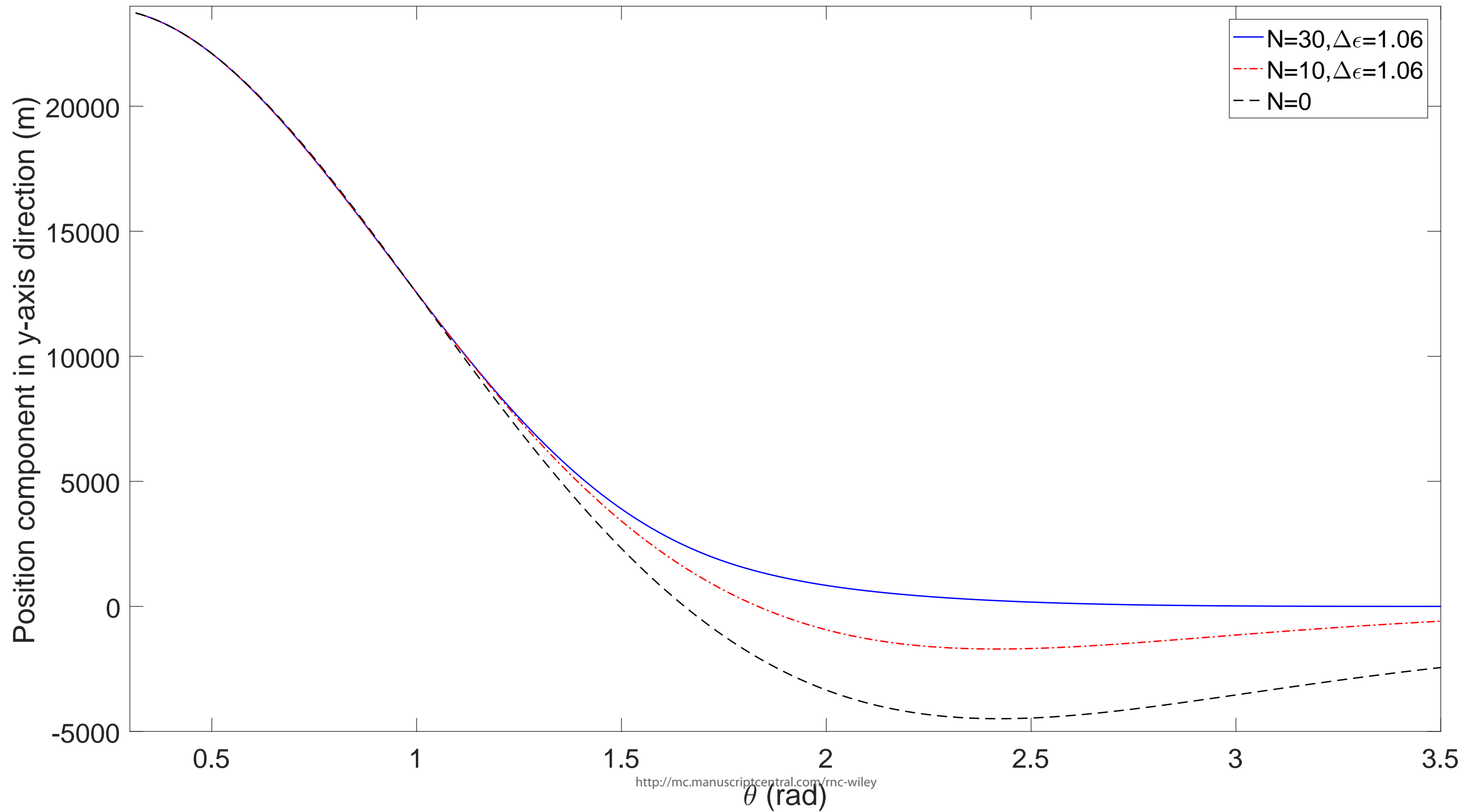
1
2
3
4
5
6
7
8
9

<http://mc.manuscriptcentral.com/rnc-wiley>

1
2
3
4
5
6
7
8
9
10
11
12
13
14
15
16
17
18
19
20
21
22
23
24
25
26
27
28
29
30
31
32
33
34
35
36
37
38
39
40

Position component in x-axis direction (m)

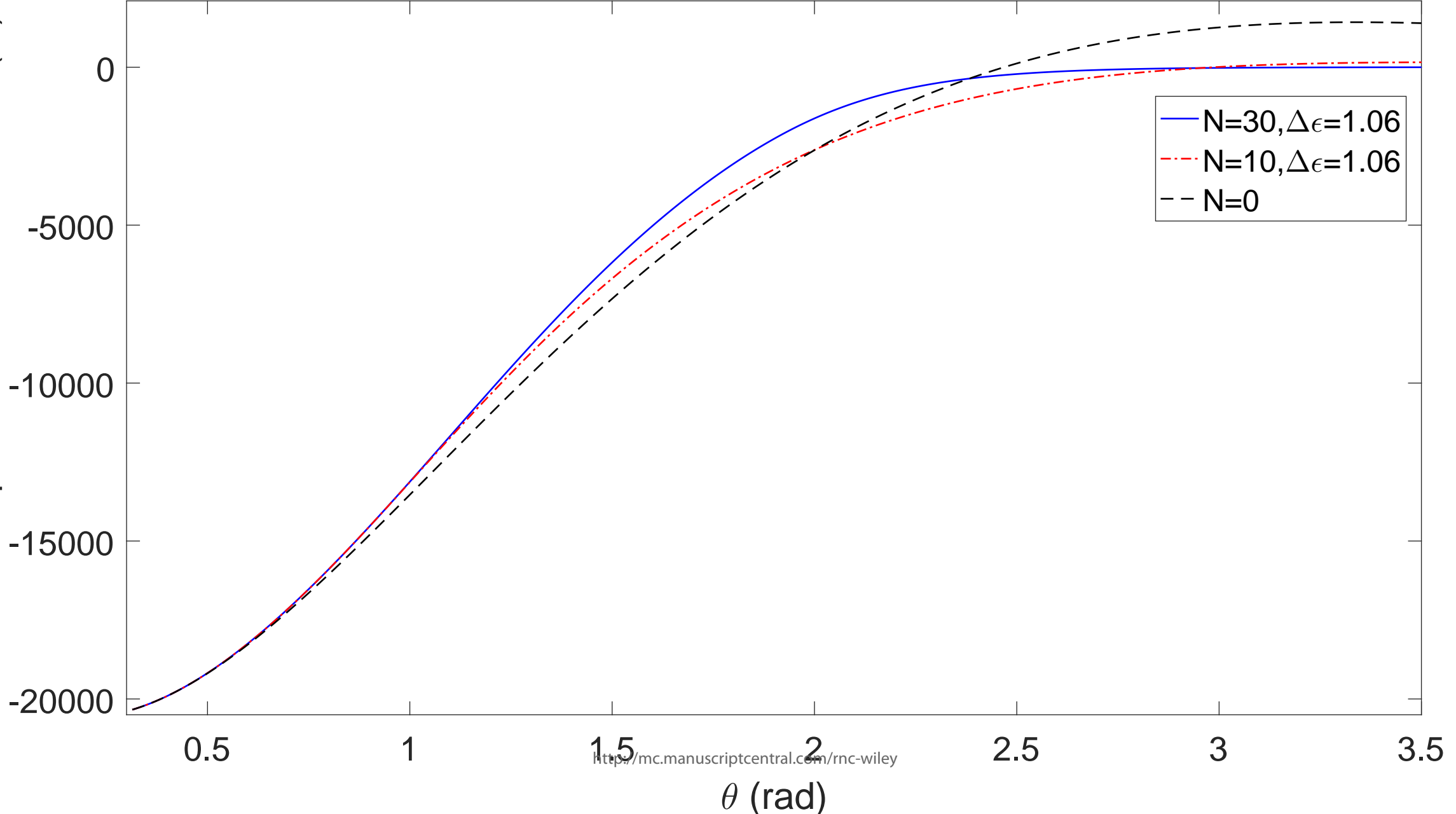


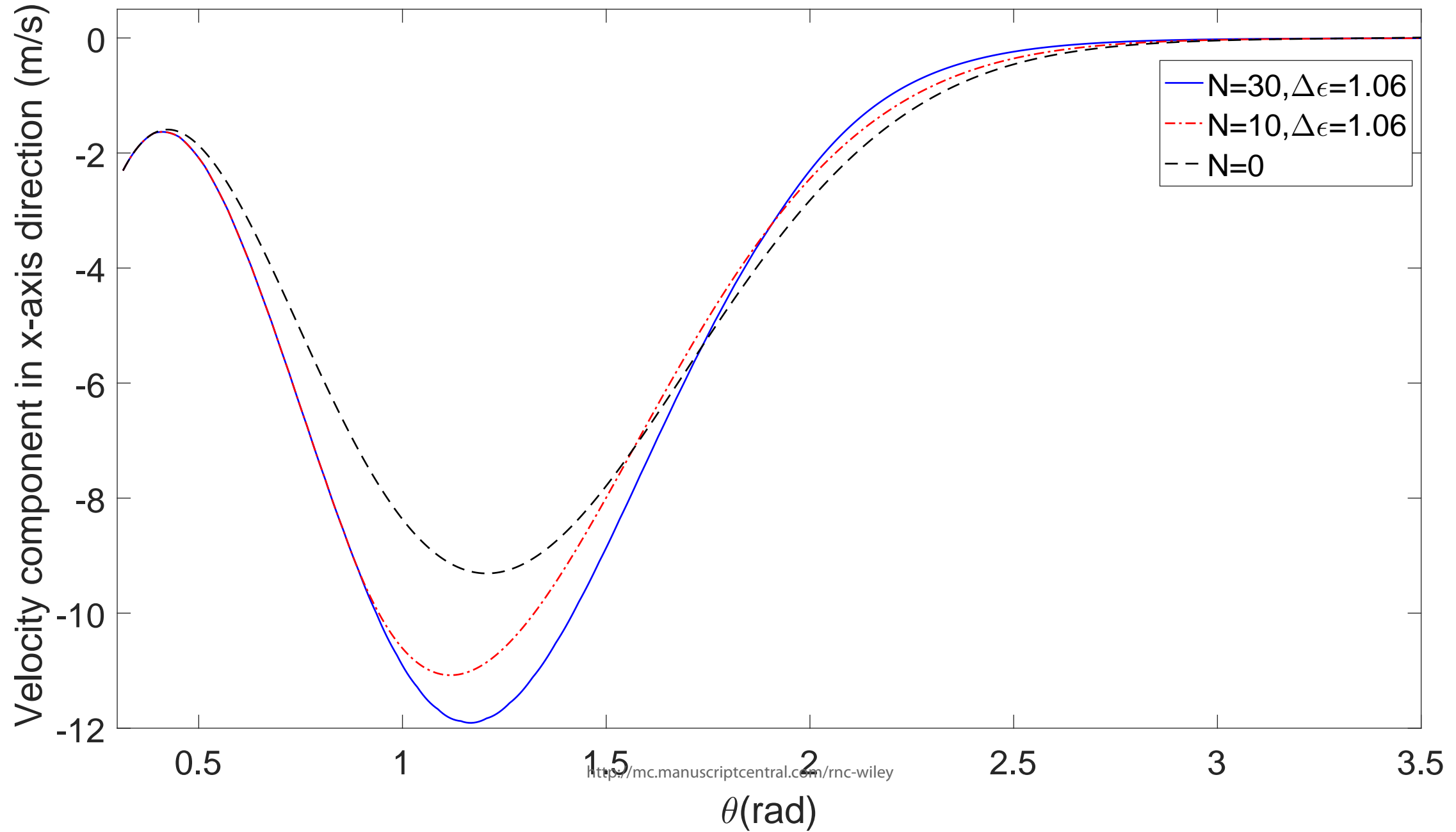


1
2
3
4
5
6
7
8
9
10
11
12
13
14
15
16
17
18
19
20
21
22
23
24
25
26
27
28
29
30
31
32
33
34
35
36
37
38
39
40
41
42
43
44
45
46
47
48
49
50
51
52

Downloaded from <https://onlinelibrary.wiley.com/doi/10.1002/rnc.6509> by Curtin University Library, Wiley Online Library on [08/04/2024]. See the Terms and Conditions (<https://onlinelibrary.wiley.com/terms-and-conditions>) on Wiley Online Library for rules of use; OA articles are governed by the applicable Creative Commons License

1
2
3
4
5
6
7
8
9
10
11
12
13
14
15
16
17
18
19
20
21
22
23
24
25
26
27
28
29
30
31
32
33
34
35
36
37
38
39
40

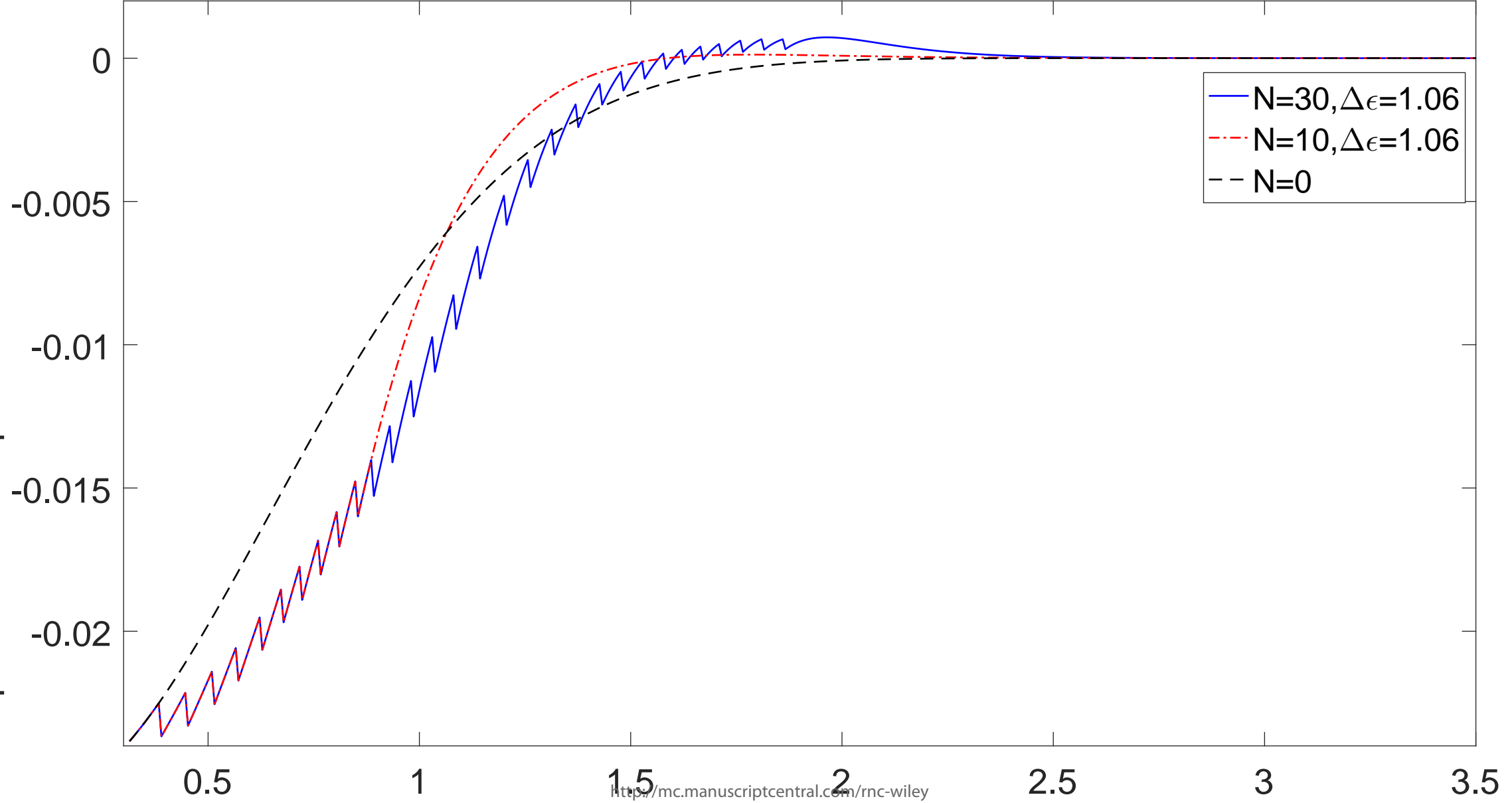




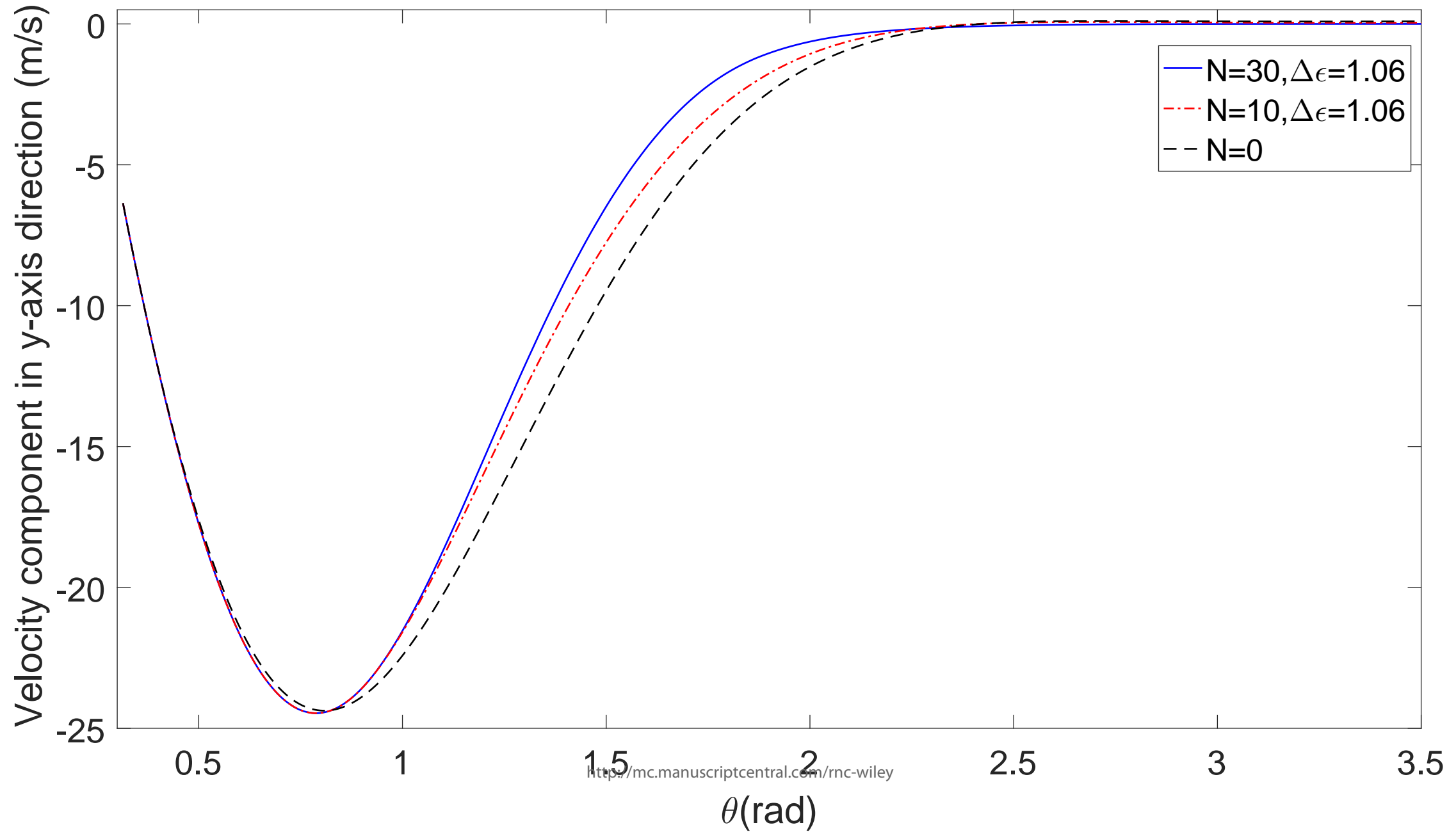
Author Manuscript

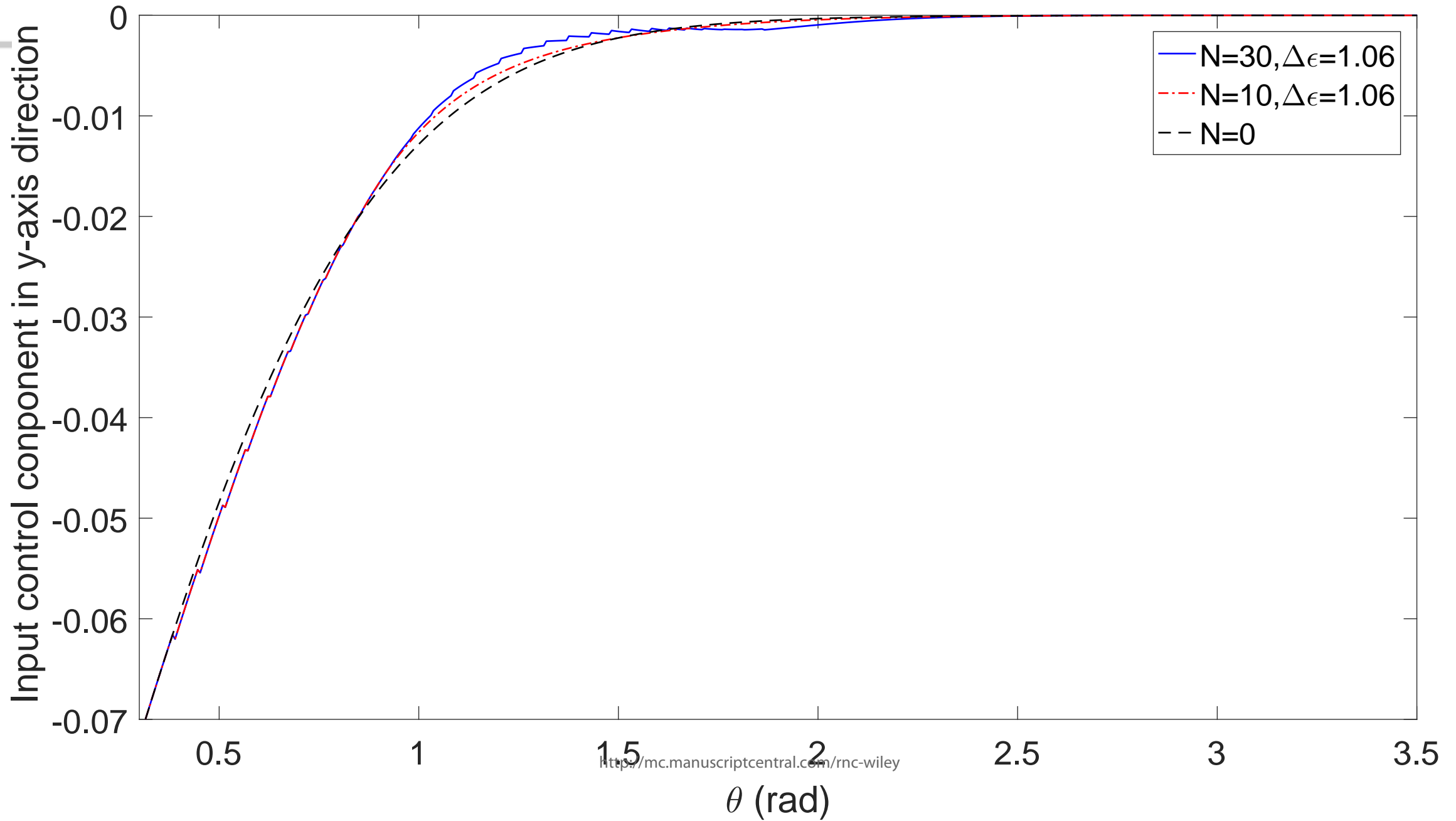
1
2
3
4
5
6
7
8
9
10
11
12
13
14
15
16
17
18
19
20
21
22
23
24
25
26
27
28
29
30
31
32
33
34
35
36
37
38
39
40

Input control component in x-axis direction

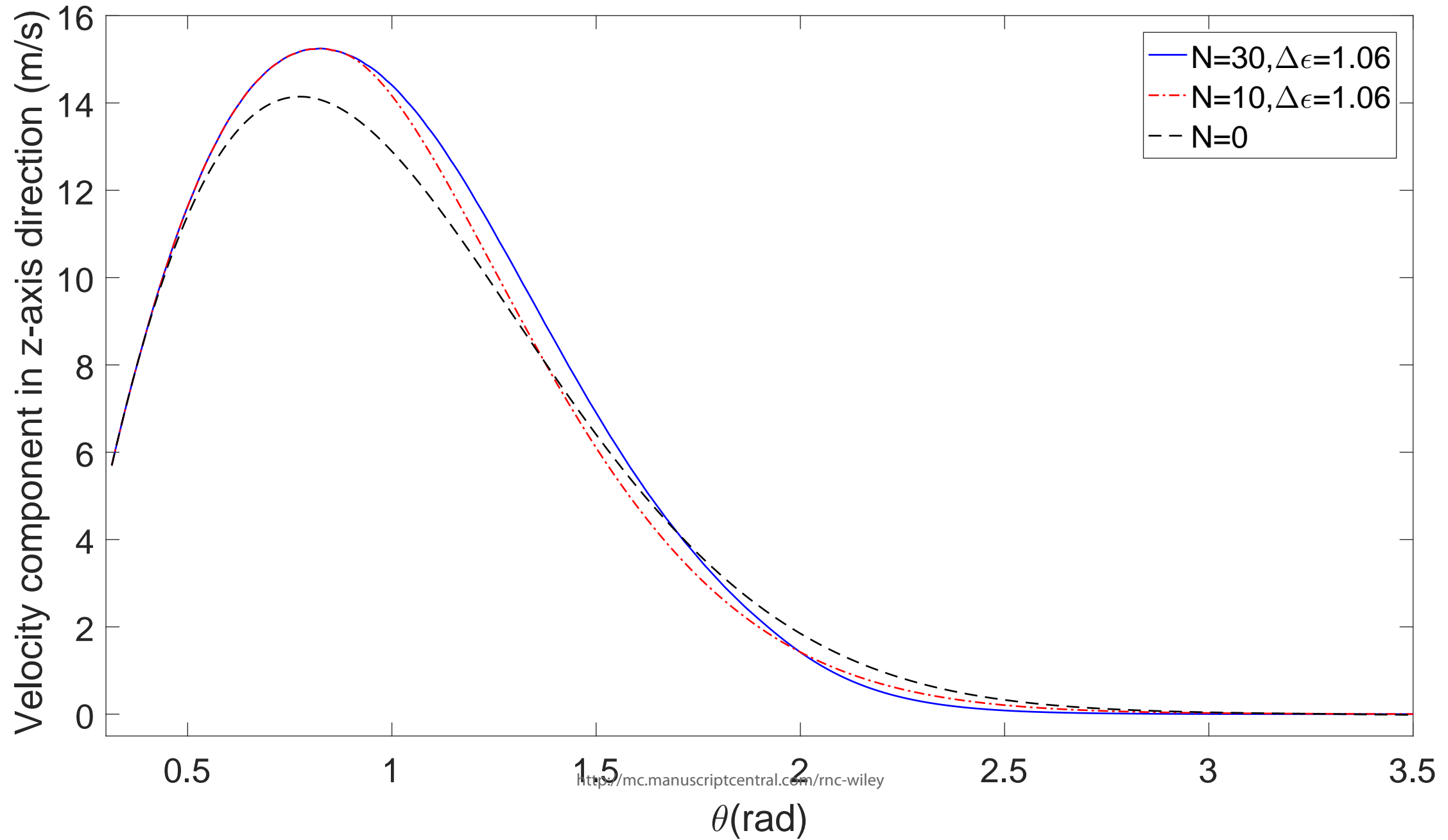


<http://mc.manuscriptcentral.com/rnc-wiley>



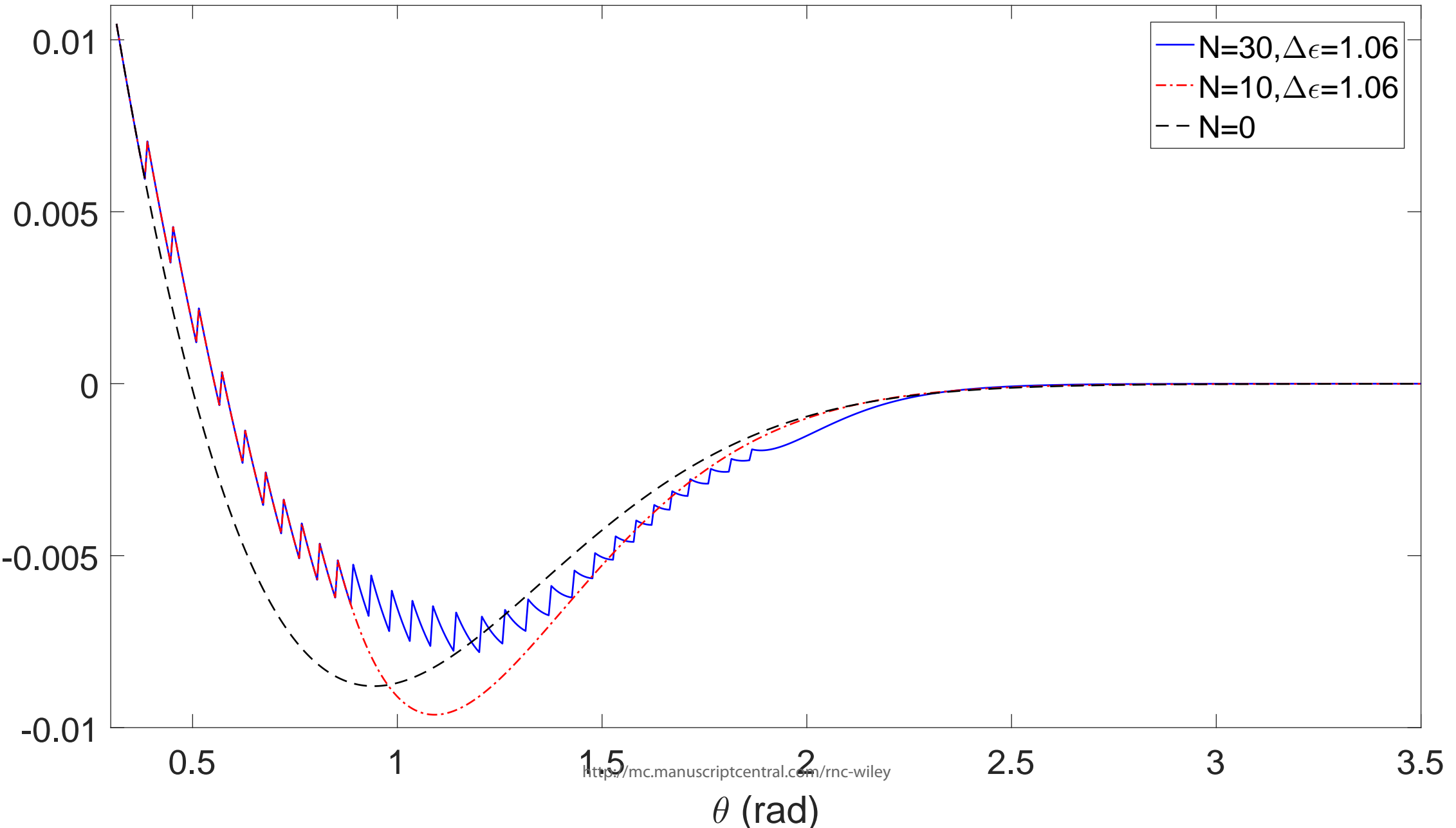


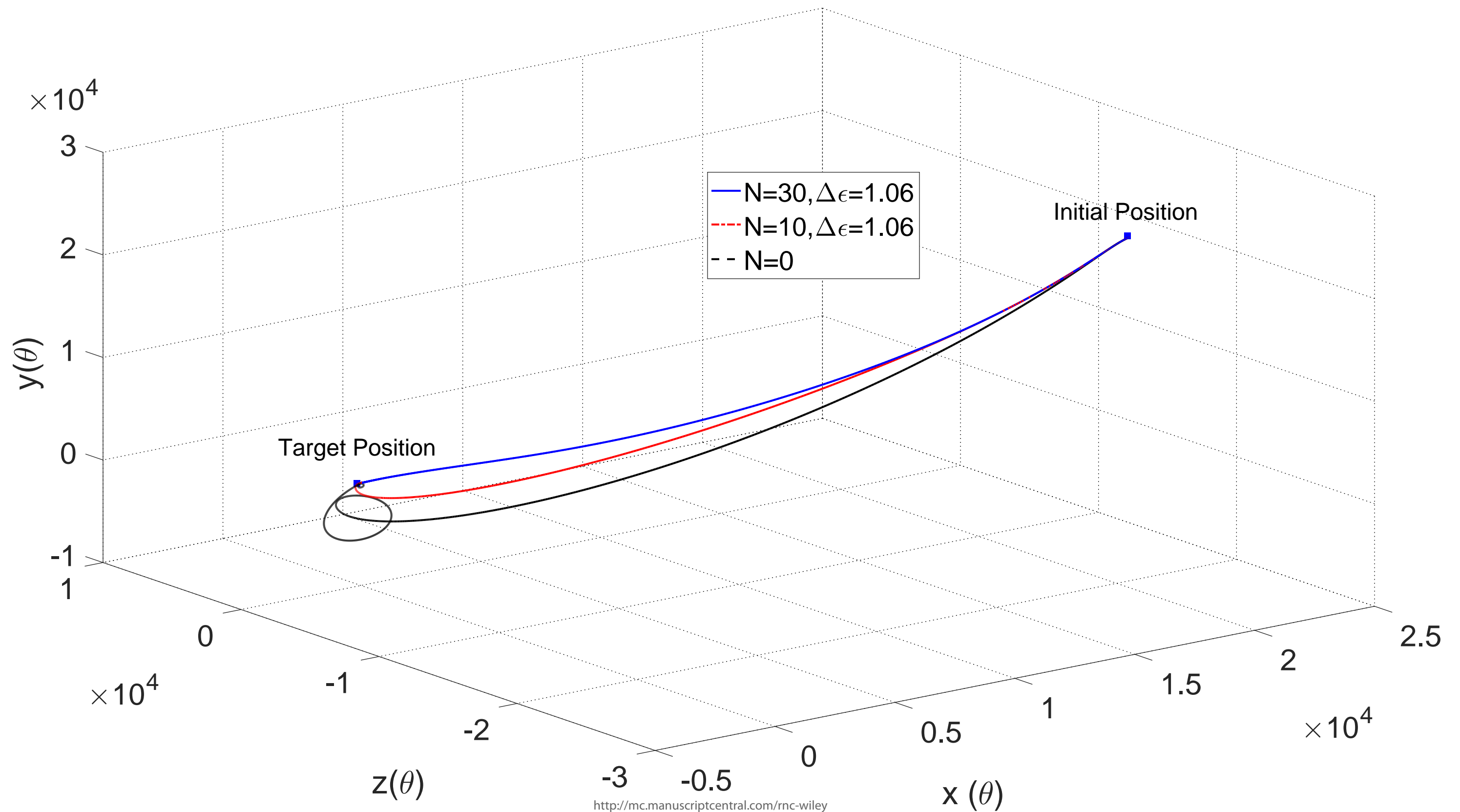
Author Manuscript



1
2
3
4
5
6
7
8
9
10
11
12
13
14
15
16
17
18
19
20
21
22
23
24
25
26
27
28
29
30
31
32
33
34
35
36
37
38
39
40

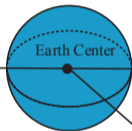
Input control component in z-axis direction



1
2
3
4
5
6
7
8
9
10
11
12
13
14
15
16
17
18
19
20
21
22
23
24
25
26
27
28
29
30
31
32
33
34
35
36
37
38
39
40
41
42
43
44
45
46
47
48
49
50
51
52
53
54
55Author Manuscript
1991239, 2023, 3, Downloaded from https://onlinelibrary.wiley.com/doi/10.1002/rnc.6999 by Curtin University Library, Wiley Online Library on [08/04/2024]. See the Terms and Conditions (https://onlinelibrary.wiley.com/terms-and-conditions) on Wiley Online Library for rules of use; OA articles are governed by the applicable Creative Commons License

1
2
3
4
5
6
7
8
9

Target Orbit



Earth Center

<http://mc.manuscriptcentral.com/mc-wiley>

Target Spacecraft

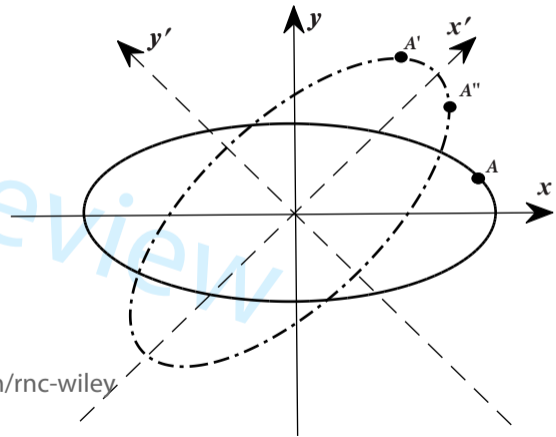
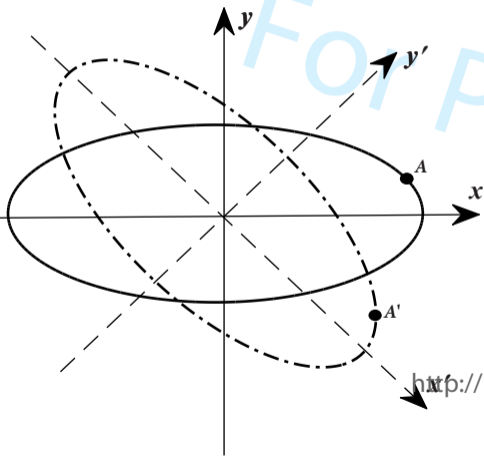
Chaser Spacecraft

$\dot{\theta}$

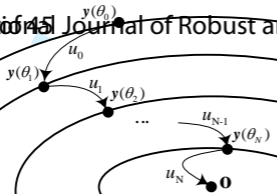
z

y

x



1
2
3
4
5
6
7
8
9



$$O(\Lambda_{\max}(\varepsilon_N))$$

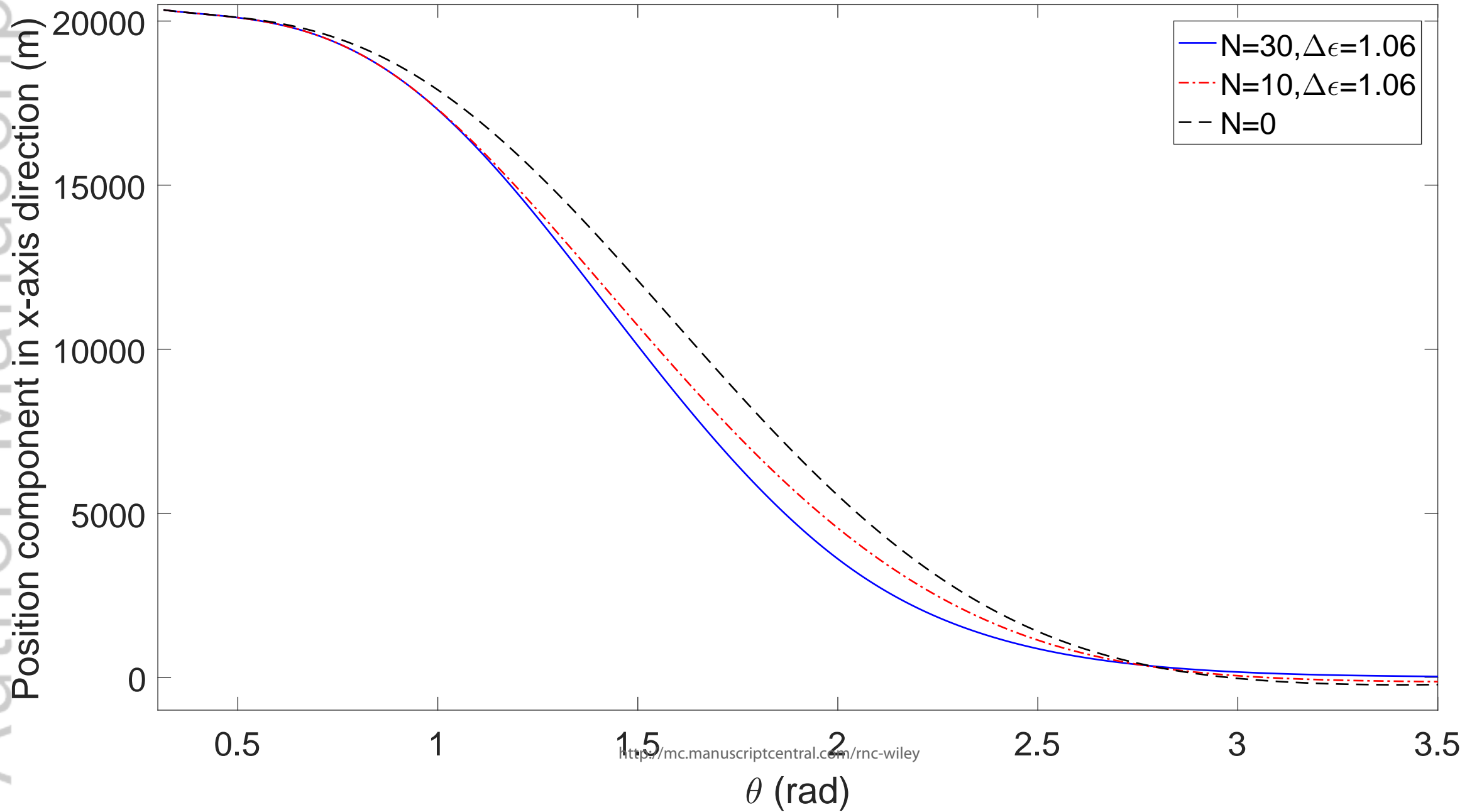
\vdots

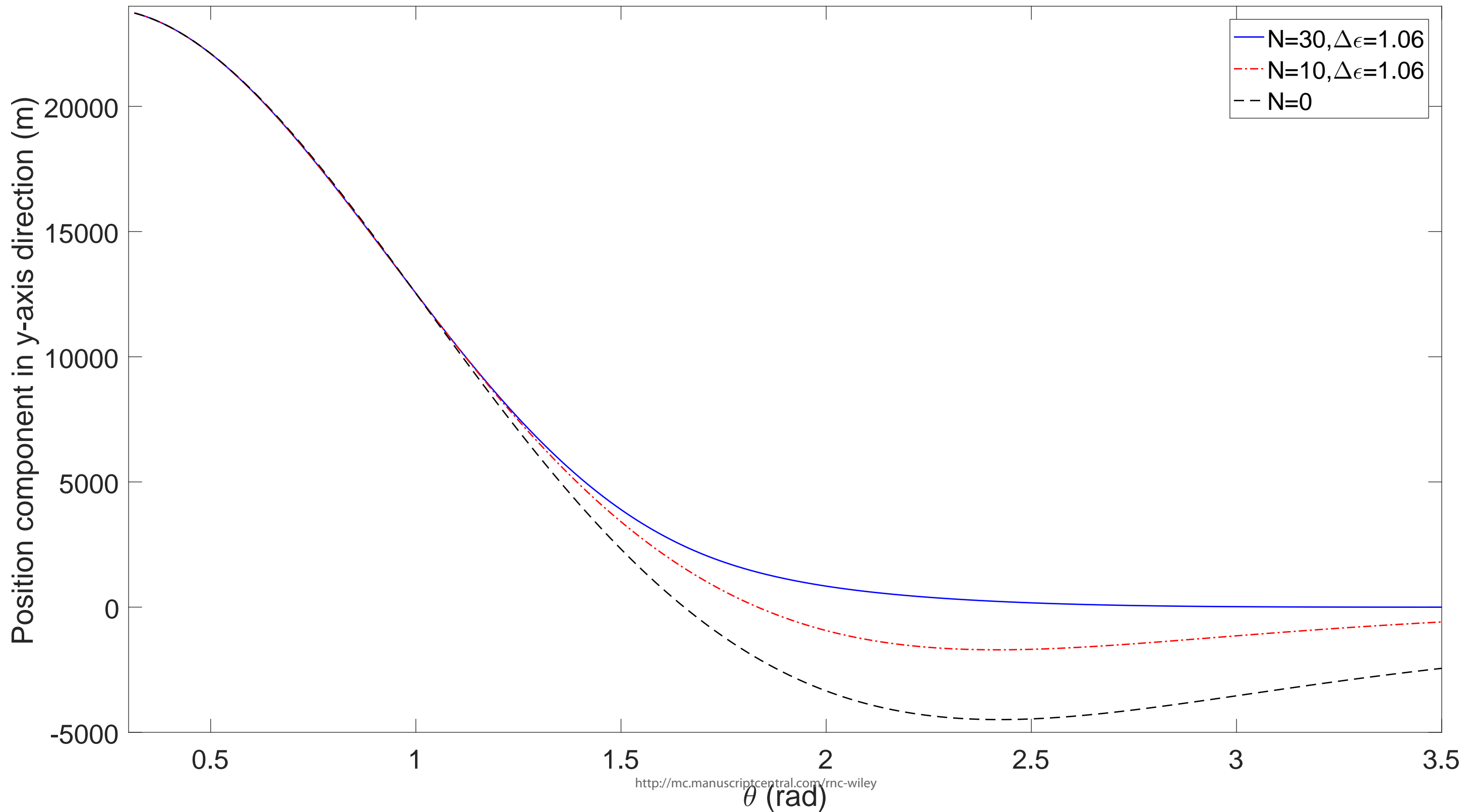
$$O(\Lambda_{\max}(\varepsilon_1))$$

$$O(\Lambda_{\max}(\varepsilon_1))$$

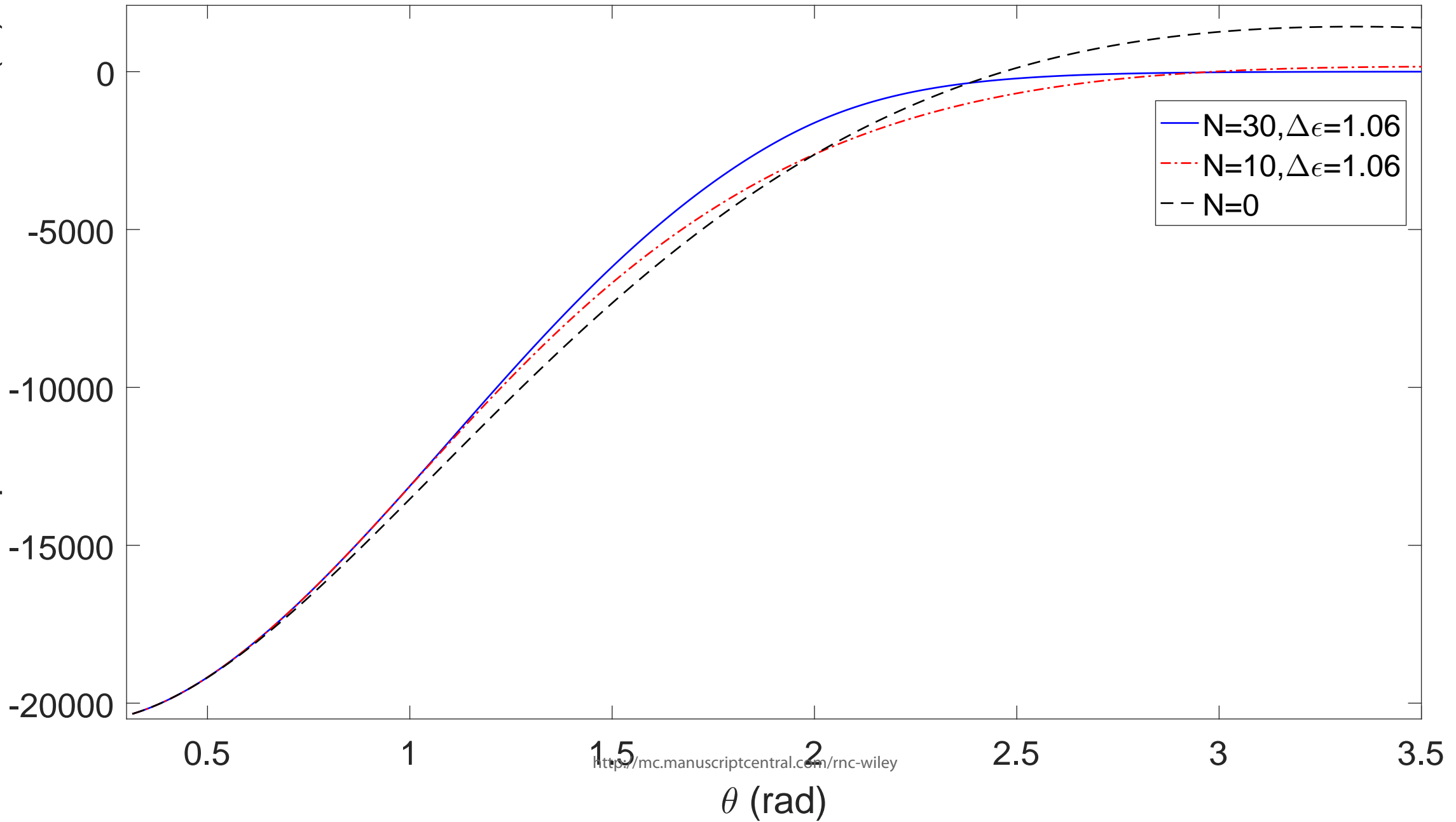
$$O(\Lambda_{\max}(\varepsilon_0))$$

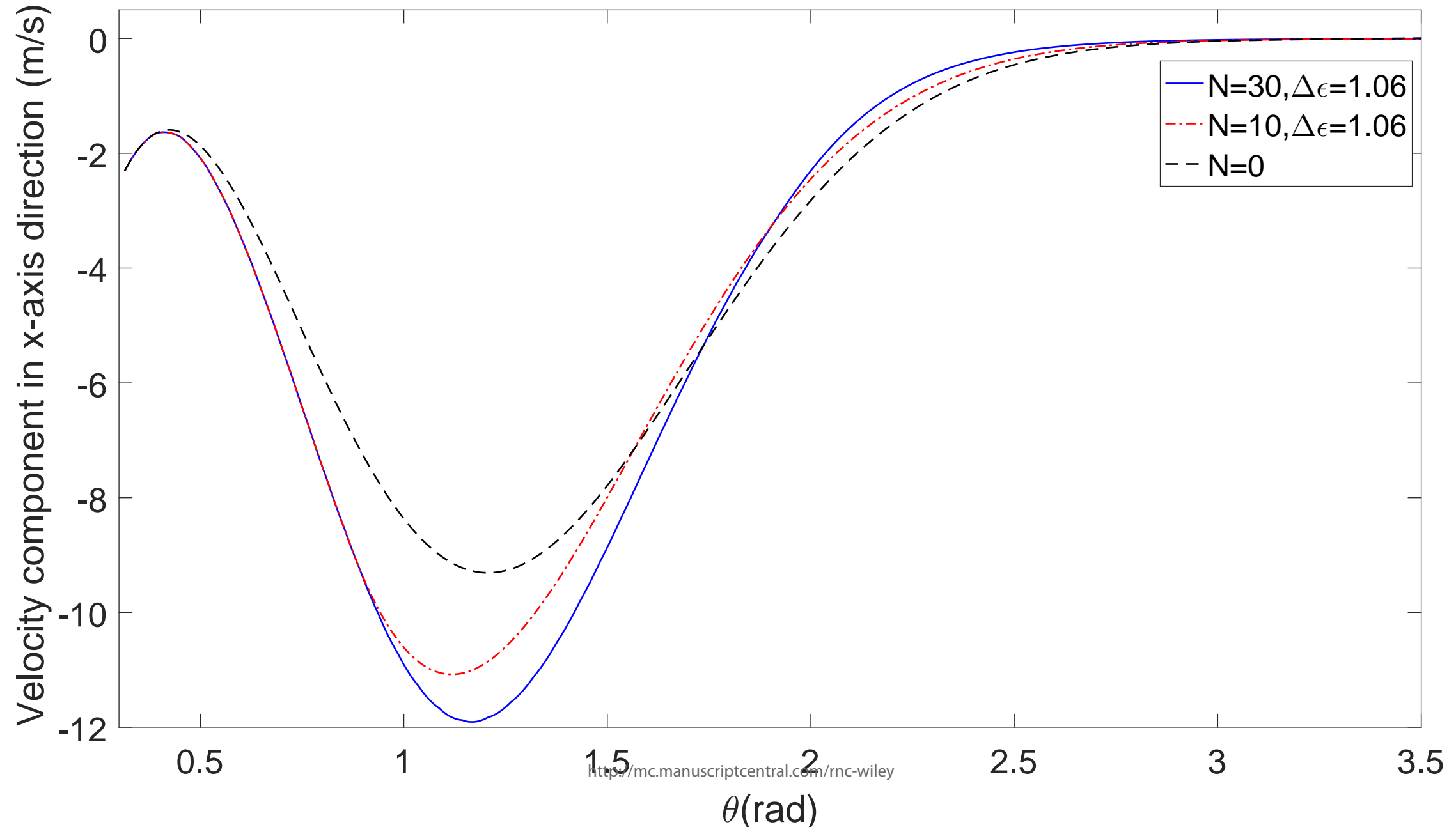
<http://mc.manuscriptcentral.com/rnc-wiley>



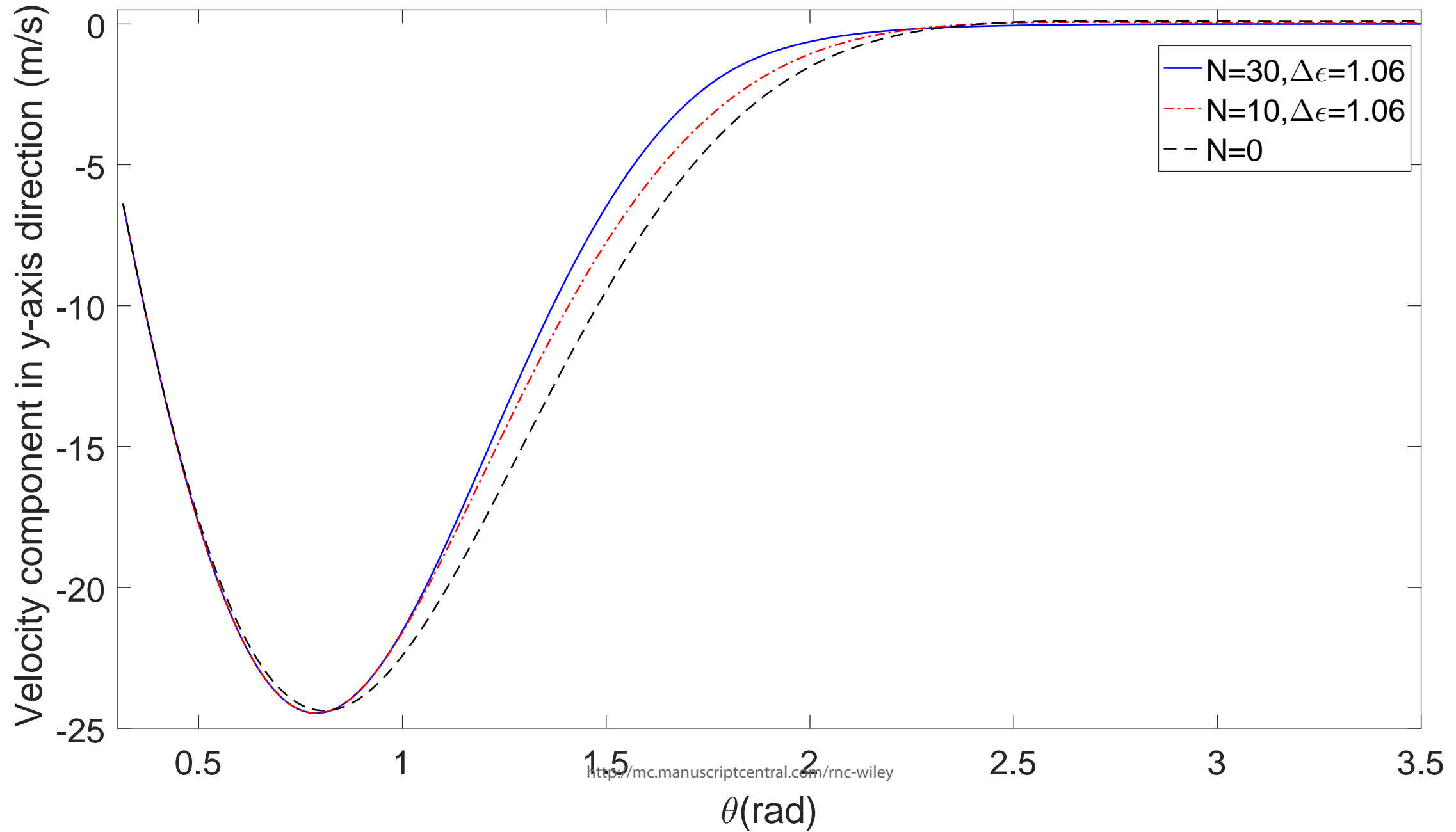


1
2
3
4
5
6
7
8
9
10
11
12
13
14
15
16
17
18
19
20
21
22
23
24
25
26
27
28
29
30
31
32
33
34
35
36
37
38
39
40
41
42
43
44
45
46
47
48
49
50
51
52



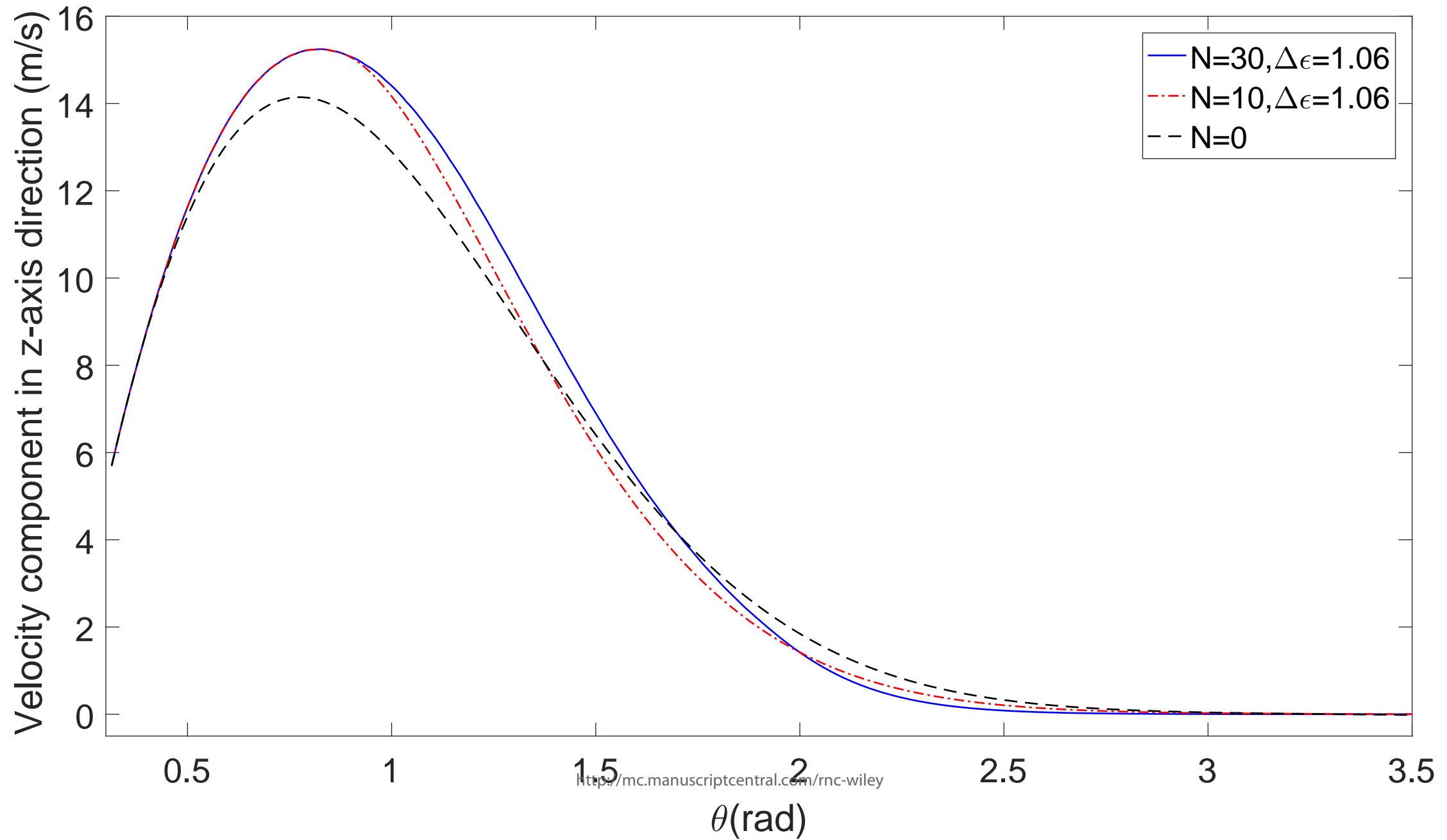


Author Manuscript



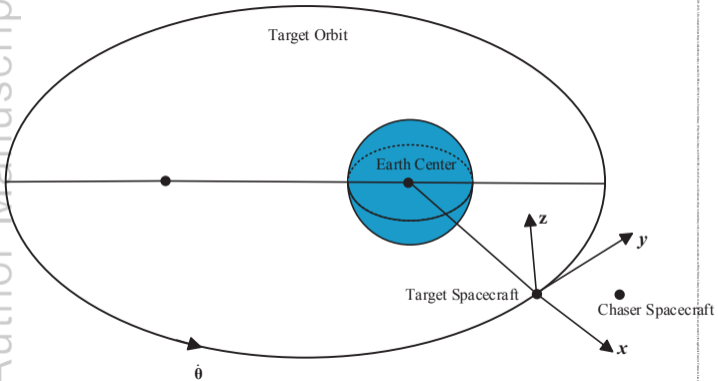
Author Manuscript

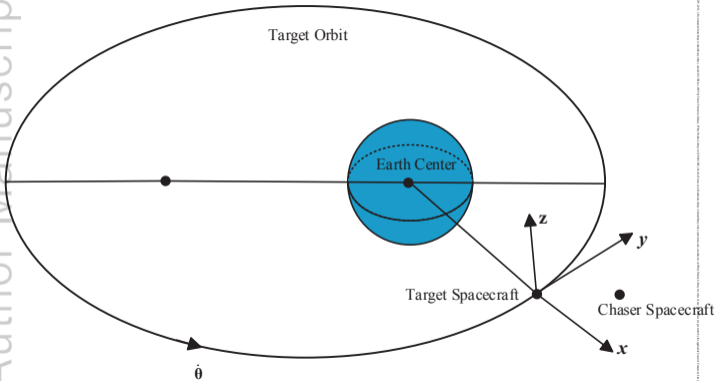
Downloaded from https://onlinelibrary.wiley.com/doi/10.1002/rnc.6079 by Curtin University Library, Wiley Online Library on [08/04/2024]. See the Terms and Conditions (https://onlinelibrary.wiley.com/terms-and-conditions) on Wiley Online Library for rules of use; OA articles are governed by the applicable Creative Commons License



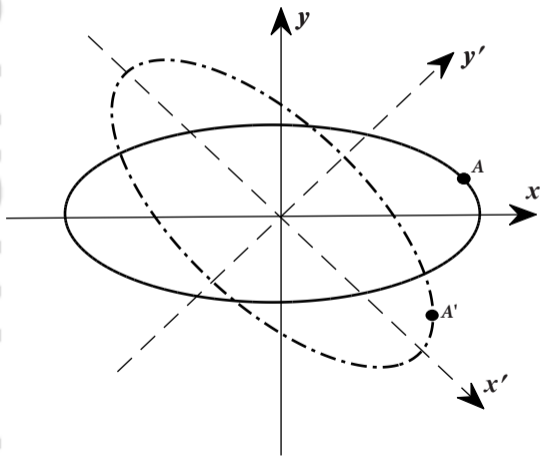
1
2
3
4
5
6
7
8
9
10
11
12
13
14
15
16
17
18
19
20
21
22
23
24
25
26
27
28
29
30
31
32
33
34
35
36
37
38
39
40

199123, 2023, 3, Downloaded from https://onlinelibrary.wiley.com/doi/10.1002/rnc.6079 by Queen University Library, Wiley Online Library on [08/04/2024]. See the Terms and Conditions (https://onlinelibrary.wiley.com/terms-and-conditions) on Wiley Online Library for rules of use; OA articles are governed by the applicable Creative Commons License

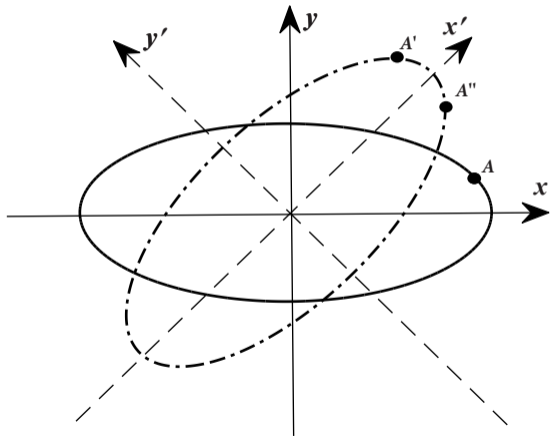




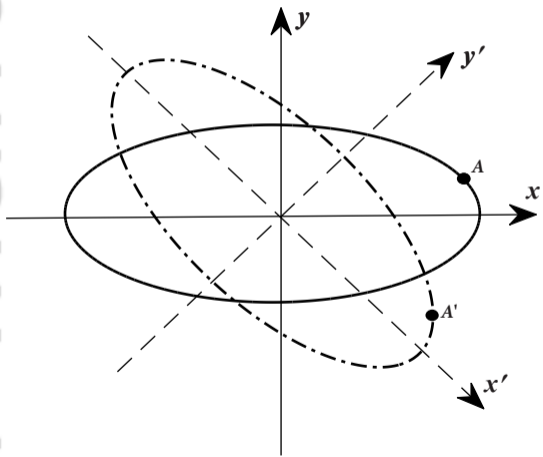
$$\det(Q)=1$$



$$\det(Q)=-1$$



$\det(Q)=1$



$\det(Q)=-1$

